REPUBLIC OF TÜRKİYE

ALTINBAŞ UNIVERSITY

Institute of Graduate Studies

Electrical and Computer Engineering

MINIATURIZED COPLANAR WAVEGUIDE-FED UWB ANTENNA FOR WIRELESS APPLICATIONS

Maryam JAMEEL

Doctor of Philosophy

Supervisor

Assoc.Prof. Dr. Doğu Çağdaş ATİLLA

Istanbul, 2023

MINIATURIZED COPLANAR WAVEGUIDE-FED UWB ANTENNA FOR WIRELESS APPLICATIONS

Maryam JAMEEL

Electrical and Computer Engineering

Doctor of Philosophy

ALTINBAŞ UNIVERSITY

2023

The dissertation titled MINIATURIZED COPLANAR WAVEGUIDE-FED UWB ANTENNA FOR WIRELESS APPLICATIONS prepared Maryam JAMEEL and submitted on 19/04/2023 has been **accepted unanimously** for the degree of Ph.D. in Electrical and Computer Engineering.

____

Assoc. Prof. Dr. Doğu Çağdaş ATİLLA

Supervisor

Thesis Defense Committee Members:

Assoc. Prof. Dr. Doğu ÇAĞDAŞ ATİLLA	Department of Electrical and Electronics Engineering, Altınbaş University	_____________
Assoc. Prof. Dr. Yasa EKŞİOĞLU ÖZOK	Department of Electrical and Electronics Engineering, Altınbaş University	_____________
Asst. Prof. Dr. Muhammad ILYAS	Department of Computer Engineering, Altınbaş University	_____________
Asst. Prof. Dr. Cahit KARAKUŞ	Department of Computer Engineering, Esenyurt University	_____________
Asst. Prof. Dr. Çağatay AYDIN	Department of Electrical and Electronics, Ege University	_____________

I hereby declare that this dissertation meets all format and submission requirements of a Ph.D. dissertation.

Submission date of the thesis to Institute of Graduate Studies: __/__/___

I hereby declare that all information/data presented in this graduation project has been obtained in full accordance with academic rules and ethical conduct. I also declare all unoriginal materials and conclusions have been cited in the text and all references mentioned in the Reference List have been cited in the text, and vice versa as required by the abovementioned rules and conduct.

Maryam JAMEEL

Signature

DEDICATION

I would thank my family especially (my husband, father, mother, and sisters) for their support in this journey and thank my daughter for sharing this experience from the first month in my womb until now with her first-year-old.

ABSTRACT

MINIATURIZED COPLANAR WAVEGUIDE FED UWB ANTENNA FOR WIRELESS APPLICATIONS

JAMEEL, Maryam

Ph.D., Electrical and Computer Engineering, Altınbaş University,

Supervisor: Assoc.Prof. Dr. Doğu Çağdaş ATİLLA

Co-Supervisor: Assoc. Prof. Dr. Yaqeen S. Mezaal

Date: April / 2023

Pages: 72

There has been a discernible increase in the number of attempts made over the course of the past few years to both reduce the dimensions of ultra-wideband (UWB) antennas and their bandwidth. These two ideas, the first of which involves adding slots to the patch radiator or ground planes, have the potential to successfully handle the problem of a microstrip antenna's restricted bandwidth. This can be accomplished by adding slots to the patch radiator or ground planes. A compact monopole antenna design that is based on Locked-Key topology has been introduced. This design makes use of a FR4 substrate and is fed by a coplanar waveguide (CPW). The purpose of this is to achieve the goals that were stated earlier. This design is presented in two separate styles, each of which has a different slot shape in the radiating patch. Both styles are shown below. It functions within an extremely broad spectrum that spans a frequency range of 3.581 to 14 GHz and has a bandwidth of 10.354 GHz. Additionally, the frequency range that it covers is extremely broad. The overall dimensions are 25 by 27 millimetres squared. The antenna that is being discussed here has the same dimensions as those that were mentioned earlier; however, it has an impedance bandwidth of 10 GHz, spanning from 3.27 to 13.27 GHz. The second configuration of this antenna has been described. Radio networks of all kinds, including ultra-wideband (UWB) and others, can benefit from its implementation. The electromagnetic software that was developed by CST was utilized so that the performance of the antenna design could be simulated and investigated. The final design format we have compared the proposed antenna to a number of studies that have been published in the scientific literature, and as a result of this comparison, we have found that the proposed antenna has the smallest size while also possessing the highest bandwidth of all of the verified research. After the antenna has been constructed, the results of the simulation and the ones that were actually observed are compared and correlated with one another. This study presents and analyses a brand-new ultra-wideband (UWB) slanted patch antenna. The UWB stands for ultra-wideband. During operation, the antenna is supported by an FR-4 substrate that has dimensions of 27.2 millimetres by 14 millimetres by 1.5 millimetres and a permittivity value of 4.3. The innovative antenna design that we have developed includes as some of its characteristics a Ground Plane on FR4 Substrate, Four Stage Stepped Impedance Resonators (FSSIR), and a Slotted Patch Resonator as part of its construction. The examination of the responses to the S11 questionnaire revealed that the frequency range is somewhere between 2.91 and 9.13 GHz. During the construction of the antenna, a prototype built in CST Microwave Studio was utilized. It is conceivable that the use of this technology will also assist in the operation of other radio communication systems. The outcomes of the S11 simulations and the real-world measurements are very similar to one and quite consistent with one another.

Keywords: MPA, Energy Harvesting, Antenna, UWB, Rectenna.

TABLE OF CONTENTS

LIST OF TABLES

Pages

LIST OF FIGURES

Pages

ABBREVIATIONS

WAN : Wide Area Networks
LAN : Local Area Networks
FCC : Federal Communications Commission
UWB : Ultra-Wide Band
CPW : Coplanar Waveguide
FSS : Frequency Selective Surface

1. INTRODUCTION

1.1 INTRODUCTION

Wireless communication, which does away with the need for cables, offers users a broad variety of communication services regardless of location. These services can be utilized at home, on an airplane or ship, in a university, and in many other places. There is still the possibility of using wired communication services and capabilities [1]. Wire-based computer networks such as Metropolitan Area Networks (MAN), Wide Area Networks (WAN), Local Area Networks (LAN), and Wireless Local Area Networks (WLANs) are a few instances of these (commercially known as Wi-Fi and WiMAX). Ever since the beginning of time, people have understood the significance of being able to communicate with one another despite physical boundaries separating them. electromagnetic radiation traveling around the planet via their propagation in the atmosphere [2]. After going through that, I was able to broaden my perspectives in terms of communication. In recent years, there have been significant advancements in antennas, specifically in terms of operating systems, device size, and strategies for improving the performance of wireless networks. One of the most fundamental parts of wireless gadgets is the antenna. As a direct consequence of this, the demand for antennas has skyrocketed. The size and weight of portable devices continue to decrease, and as a result, antennas that are easily incorporated with radio frequency beams are becoming an increasingly important component. In light of this, antennas that are capable of covering a broad spectrum of wireless communication wavelengths have taken on a greater level of significance in recent years [3]. Antennas are essential for transmitting and receiving electromagnetic radiation and are required in both cases. Microstrip antennas are a common option for use in contemporary communication systems due to their small size, high efficiency, and the fact that their radiating components can be customized at a low cost. Microstrip antennas are not appropriate for future communication networks for a number of reasons, the most important of which are their low gain and limited bandwidth, both of which need to be addressed. In the most recent few years, there has been a significant increase in desire for the Ultra-Wideband system. The United States Federal Communications Commission (FCC) describes ultra-wideband (UWB) as a radio system that has a bandwidth that is greater than 25 percent of the central frequency and operates between 3.1 and 10.6 gigahertz. UWB antenna design should take into account a number of important factors, including adaptability to impedance, radiation stability, small size, and reduced cost [4]. UWB technology has a number of benefits, including a low interference rate, a high data rate, security, a cheap cost, and a low level of complexity. The fact that the stimulus lasts for such a short amount of time (less than one nanosecond) and that precise time synchronization of the receptors is required is a limitation of this technology. This technology is used in a broad variety of different applications.

UWB devices should really function at a core frequency that is 20 percent higher, despite the fact that they are described as having bandwidths that are greater than or equal to 500 MHz in fractional bandwidth. Printed antennas have proven to be a feasible option due to the ease with which they can be produced and integrated into microwave systems. This makes them an attractive choice. As a general guideline, coplanar waveguides are utilized in the process of providing power to antennas (CPW). Patches are able to be divided thanks to the use of two drivers as separators. The earth and patch are completely surrounded by three conductors that are placed on top of the substratum. Alterations are made to the parameters of the UWB application on the same antenna [5]. CPW feed antennas are seeing more and more use in modern wireless communication systems due to the ease with which they can be integrated with MMIC circuits, the reduced radiation loss they experience, and the less spread they experience in comparison to microstrip antennas. A straightforward open CPW transmission line can be converted into an antenna by making modifications to either the signal stripe or the ground plane. The breadth of the ground plane, the length of the signal strip, and the distance between them are all factors that can influence the radiation parameters of a CPW-fed antenna. [6]. In recent years, there has been an explosion of creativity in terms of design for dual band antennas. The word "energy harvests" is used to describe various methods that combine the production of energy with its storage. There are a variety of applications for environmental energy, in addition to other kinds of non-thermal energy. Printed antennas are ideal for energy harvesting because of their low cost, compact size, low weight, and flat structure. Additionally, they are ideal because they are ideal for energy harvesting. In light of this, manufacturers and researchers alike are showing a significant amount of interest in high-bandwidth rectangular antennas that are also relatively inexpensive. 1990 was the year that saw the first mention of a CPW-fed antenna. Rather than using a coplanar waveguide, a slot antenna should be used. In addition to the compact tapered-slot antenna and the circular patch CPW supplied circularly polarized antenna, there are a variety of other antenna types that could be utilized for a variety of applications. These antennas come in a wide range of sizes and shapes. These kinds of radiating structures are difficult to construct, and even if they are successful, the bandwidths they produce are considered insufficient and are only helpful in a limited number of circumstances. It is challenging to construct a CPW-fed antenna that has a broad frequency, a straightforward radiating structure, and favourable efficiency as well as radiation patterns [7]. CPW and microstrip line feeders are the most prevalent types of feed used for monopole antennas. On the other hand, CPW feeding is recommended because the ground plane and the radiator's components are virtually indistinguishable from one another. In contrast to the microstrip line feeder, the CPW-fed antenna requires that the antenna have a ground plane in order for monolithic microwave integrated circuits to be readily coupled to the antenna [8].

1.2 LITERATURE REVIEW

Antenna types based on UWB have been the subject of significant research and documentation in published works. Some of these antenna types are included below for your convenience. There are a lot of different methods to increase the gain of the antenna. These techniques include reflecting metal patches, parasitic, folding the ground plane into itself, suspending the ground and metamaterial superstrates, introducing apertures, and folding the ground plane into itself. It is possible to achieve greater gains by incorporating parasitic components [9]. Six cylinders were utilized in the construction of the spreading element in the shape of a strawberry. Because of this, the antenna's UWB frequency spectrum was able to be increased. On a substrate made of FR4, an antenna with a bandwidth of 8.85 GHz (3.05–11.9 GHz) was projected using CPW feeding. This antenna covered the entire allowable frequency spectrum for UWB transmissions. Gains of 6.22 dB were obtained in both the lower and higher bands using the UWB SAPM antenna in conjunction with the FSS reflector. The dimensions of the antenna are as follows: 61 on 61 on 1.6 mm3. Applications such as ground-penetrating radar (GPR) and ultra-wideband (UWB) radio can both make use of the recommended antenna construction because of the antenna's directed and balanced far-field pattern [l0]. The antenna has a frequency range that extends from 1.76 GHz all the way up to 11.07 GHz, but it is insensitive to frequencies that fall between 2.42 GHz and 5.37 GHz. Gain and efficiency of the antenna are constant across the entire operating spectrum, with the exception of the band that has been notched off, which is not depicted in these simulations. The antenna that is being demonstrated may prove useful to future wireless communication systems in the future. Using a simple CPW-fed antenna, it is feasible to operate on both bands simultaneously. Harmonics in electromagnetic bands can be reduced with the assistance of structures that make use of rectangular lattices. EBG structures, in addition to providing band-stopping properties, served to expand the antenna's optimal operating bandwidth, which was a significant benefit. EBGs have a large frequency bandgap and a high surface impedance, which causes them to generate a ring of reflection that is in phase with the wave that is incident upon them. The surface area of the small slot antenna can be made smaller by combining rectangular lattice EBGs in a CPW feeding line [11]. Monopole antennas with increased gain and improved efficiency have been developed in the paper [12]. This broadband printable monopole antenna was used in conjunction with our CPW so that we could put our method of antenna design to the test and make any necessary improvements. The use of FR-4 substrates is an option that minimizes expenses when it comes to the construction of wireless communication systems. When it is functioning at the pinnacle of its effectiveness, the UWB antenna achieves a maximal output gain of 4.1 dB. In paper [13], the authors discuss research that has improved antenna gain by using frequency-selective surface (FSS) techniques for ultra-wideband (UWB) frequencies. The taxonomy of the research landscape was utilized in order to locate the method of increasing antenna gain that was found to be the most successful. During the course of this research, the use of FSS as a deflector at UWB frequencies was also investigated. The ability of the FSS to protect against unwanted and rejected radiation while simultaneously protecting against power loss in inappropriate antenna transmission zones can be beneficial to a broad variety of applications. An illustration of a dual-spectrum device can be found in [14]. This particular device is a low-profile ISM/UWB split ring monopole. The monopole has the ability to operate in the ISM frequency range as well as the UWB frequency range at the same time. Split-ring radiators that have a circular cross-section have been employed so that the highest possible performance can be attained across both frequency bands. By coupling the two bands together, it is possible to generate frequencies in the UWB quasi-resonant range. Even though it only has two radiators, the antenna is able to reverberate in the 2.45 GHz ISM band thanks to a short stub that is incorporated into it. For use in UWB applications, high-gain and directional planar antennas that make use of FSS unit cells have been suggested [15]. There has been a presentation of a concept for an antenna that is based on the Mercedes artistic-shaped planar (MAP) antenna. The bandwidth of the antenna was increased by arranging three straight legs in a circular configuration. It was determined that a circular loop architecture along with two parallel conductive metallic patches would be used to simulate the FSS. The FSS was able to provide a stopband filter response of 10.5 GHz for frequencies ranging from 2.22 GHz to 12.7 GHz, while maintaining a bandwidth of 10.5 GHz. In terms of its physical dimensions, the FSS was only 5 millimetres broad, 5 millimetres high, and 1.6 millimetres thick. This included the antenna. It was reported that a relatively small broadband antenna was used in a variety of wireless situations in [16]. On a substrate made of dielectric FR4 with global measurements of 50 mm x 50 mm x 1.6 mm3, there are Vicsek slots and a reduced ground plane that have been printed. WiMAX and WLAN both provide bandwidth for broadband connections at frequencies spanning from 2.3 to 2.5 GHz, 3.3 to 3.5 GHz, 5 GHz, and 5.5 GHz. The effectiveness of the antenna at resonant frequencies is 88.5 percent for the E plane and 84.6 percent for the H plane, respectively, with gains of 2.78 dB and 5.32 dB. The authors demonstrated how a UWB antenna mounted on a solar panel could potentially harvest electromagnetic waves from space and transform them into electricity using a transparent cone-top tapered slot antenna that operated between 2.2GHz and 12.1GHz. The antenna generates a pattern that is characteristic of a UWB when it is placed in this configuration, when it is sandwiched between an a-Si solar screen and a piece of glass. The radiation pattern of a UWB antenna is effectively omnidirectional when it is in a position where it is sandwiched between a solar panel and glass. When the antenna is placed on glass, it produces 18 mV DC at an input power of 10 dBm with a 2.55-GHz rectifier connected to it at a distance of 5 centimetres in free space. This occurs when the antenna is operating in free space. Because of the narrowband rectifier that was used for this investigation [17], the frequency range that can be employed for power scavenging is limited to 2.49 to 2.58 GHz. It is possible to achieve a greater bandwidth by furnishing the bottom of the broad slot with symmetrical triangular corners that taper inward. The notch band frequency, which ranges from 5–6.3 GHz, is the only frequency that the antenna's 26 by 21 mm2 area does not encompass. In order to determine whether or not the VSWR and radiation properties of the proposed cantor set of fractal wide-slot UWB antenna are accurate, measurements are currently being taken. According to the findings, the small antenna provides an impedance bandwidth that is relatively broad (2.8–10.3 GHz) in addition to outstanding radiation characteristics that include the notch band that is required for UWB applications[18]. It is necessary to use a parasitic patch in addition to the antenna patch in order to achieve the required band rejection. Over the course of its existence, the general design has been through a number of iterations during which its performance has been improved. This minuscule gadget only requires a volume of (50x40x1.6) millimetres cubed. These studies are being carried out in order to generate UWB antennas, which will be utilized in upcoming Internet of Things (IoT) applications such as off-body wireless body area networks (WBAN). A full ground plane antenna can be constructed by using a Y-shaped patch and a coplanar waveguide line. Both of these components should be laid out in the same plane. There are two distinct substrates, a Rogers RO4350B measuring 5 millimetres and a felt fabric measuring 5 millimetres each. When both substrates are used, this is accomplished by adjusting the essential dimensions of the antenna as well as the measuring characteristics such as gain, bandwidth, efficiency, and radiation pattern. This research also looks into a number of other factors that could have an impact on the radiation patterns and the reflection coefficient. When using a Y-shaped slot, the largest patch size that can be achieved on either substrate is 36 to 40 mm^2. Antenna coverage may stretch from 8 to 10 GHz. When developed on the RO4350B substrate, the antenna has a bandwidth that is approximately four times greater than when developed on felt [19]. To generate rectified DC, the antenna is connected to a full-wave rectifier circuit. At a frequency of 3.1 GHz and 4 GHz, the antenna produces the highest output voltage of 1.4 V and 1.3 V, respectively, when the RF power that is coming in is approximately 17 Bm. The data from the actual world and the predictions made by the model are completely consistent with one another. The antenna is made from bendable Kodak photo paper that is 0.5 millimetres thick and has a value of r that is equal to 2, as well as a loss tangent value that is equal to 0.0015. The CST MWS software package is utilized in order to carry out numerical calculations. The inkjet printing of conductive silver nanoparticles was used to create the antenna construction that is being demonstrated here. Researchers have discovered that it is possible to create an antenna that covers the range from 2.4 GHz to 20 GHz, with a maximum gain of 1.78 dB at 3.0 GHz and 4.04dBi at 4 GHz [20].

1.3 PROBLEM STATEMENT AND MOTIVATION

MA must be improved in terms of performance, design, and shape as a result of the growing rise of personal communication systems, such as local area wireless networks, smart highway systems, direct broadcast systems, and mobile satellite communication. More electronic gadgets are needed since there are fewer of them. Antennas must be more efficient based on data transmission speed, bandwidth, and frequency for keeping up with current developments and handle all technical challenges related with this, including supplying small-sized and high-performance antennas for use in energy harvesting applications.

1.4 AIM AND OBJECTIVES

Rectennas (energy harvesting systems) operating at ultra-wideband frequency for RF wireless energy harvesting are being developed in this thesis. The objectives are: Antenna design improvements and research into several forms of energy harvesting antennas as well as investigating and improving energy harvesting systems' RF to DC rectifying circuits. A high efficiency of RF to DC conversion can be achieved because of the RF energy harvesting antenna and the rectifying circuit.

1.5 CONTRIBUTIONS

Current research is focused on designing an ultra-wideband CPW microstrip patch antenna that is both compact and efficient. Analogous to CPW's ground-plane-free design, the antenna's proposed design is based on these features. This antenna's Locked-Key radiating patch and CPW feeder met all of the required electrical standards when built on a FR4 substrate. If you're working with single-wave circuits, then CPW is an excellent choice because it allows you to link in parallel and serial with active and passive components. In order to function well at low power levels, antenna and rectifying circuit designs have been optimized. In this operating band, the energy collecting antennas have a broadband operation and a low return loss. The input impedance of rectifying circuit designs can be set to match the 50 line impedance. Antenna performance is critical to the RF energy harvesting system's ability to operate at high efficiency. CPW and a specific patch are used to create the proposed antenna, which can be used for energy harvesting. They create a new microstrip patch antenna and a rectifier. A simple rectenna can be used to convert electromagnetic energy into DC, which can then be used to power a battery.

1.6 DISSERTATION OUTLINE

The following are the outlines of this dissertation:

Chapter Two: Antenna S11 response, radiation pattern, gain, efficiency, and bandwidth are discussed in this chapter. The MA and its feeding procedures are also depicted in this chapter.

Chapter Three: The transmission line, impedance matching, rectenna idea, and energy harvesting will all be discussed in detail in this chapter.

Chapter Four: The CST simulator is used for simulating the projected antenna in this chapter. Also, the MPA and Rectifier circuit processes.

Chapter Five: The fabricating and measurements details for the projected antennas are detailed in this chapter.

Chapter Six: Finally, this chapter summarizes the study's findings and provides the essential guidance for the development of the suggested antennas in the future.

2. ANTENNA THEORY

2.1 INTRODUCTION

There are numerous different aspects of antenna design and execution that are covered in this chapter. the antenna's parameters must be measured and recorded. among these are the antenna's emission pattern, its directivity, and its gain.

2.2 ANTENNA

Based on Institute of Electrical and Electronic Engineers, an antenna can receive or emit electromagnetic waves. Wireless communication networks rely on antennas as the transmission and reception interfaces for wireless signals. As shown in Figure 2.1, an ideal half-wavelength dipole has an electric field distribution around it.

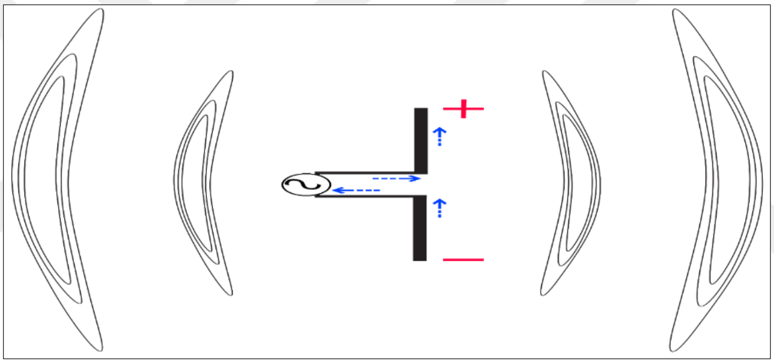

Figure 2.1: The Electric Field Distribution in a Near-Field for Dipole Antenna Parameters.

Charge builds up on the dipole's upper portion during peak positive cycles, which results in an instantaneous positive charge being generated on the dipole. These results in a negative charge being applied to the bottom half of the cell at the same time. The dotted arrows that run the length of the dipole also display the instantaneous current. As shown in Figure 2.1, the resultant radiation is produced when the time-varying source causes an oscillating charge back and forth between the dual sides for a dipole [21]. Antenna performance can be described in terms of a variety of measures, which are discussed in this section.

2.2.1 Radiation Pattern

Radiation patterns are used in physics to visualize electromagnetic power distribution in free space. The antenna's relative field strength can be inferred from these patterns, which is useful. Field measurements are performed using spherical coordinate systems, as seen in

Figure 2.2. Spherical antennas are ideal for isotropic antennas. This would be a toroid in the case of a typical dipole. A three-dimensional (3D) graph, like the one illustrated in the picture, or polar plots of horizontal and vertical cross-sections are typically used to depict the radiation pattern of an antenna. Sidelobes as well as ear lobes should be included in the diagram, as well. A good example of this is Figure 2.3 [22]. The Polar plot is a 3D radiation pattern that has been flattened.

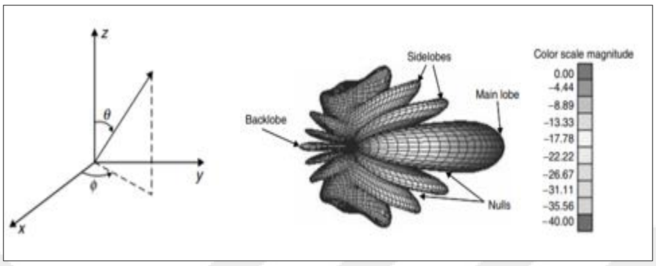

Figure 2.2: a) Spherical Coordinates, b) 3D Radiation Pattern [22].

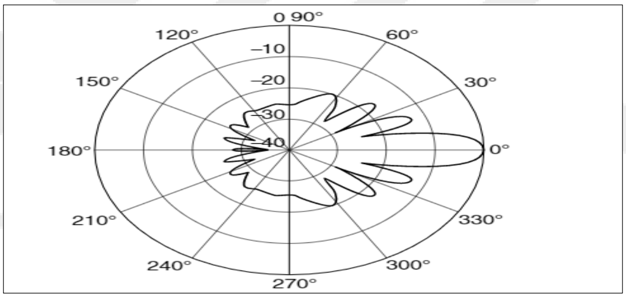

Figure 2.3: Polar plot radiation [22].

2.2.2 Directivity

The quantity of radiation that is emitted outward from an antenna in comparison to the total amount of radiation that is radiated in all directions is referred to as the "direction." The formula for determining the typical radiation intensity is to divide the overall power output of the antenna by the square of the height of the antenna (in meters). Because there has been no specification regarding the direction of the maximum intensity of the radiation, "the most intense direction is recommended." To phrase it in another way: What we mean when we talk about "directivity" is the relation of the radiation intensity in a specific direction to the radiation intensity that would be produced by an isotropic source. The following is a good way to summarize it [23]:

$$D = \frac{U}{U_0} = \frac{4\pi U}{P_{rad}} \tag{2.1}$$

In the event that the direction isn't stated, a direction of utmost radiation intensity (i.e., the highest directivity) is explained as:

$$D_{max} = \frac{4\pi U_{max}}{P_{rad}} \tag{2.2}$$

Here,

D: It stands for antenna directivity.

U: It stands for an antenna radiation intensity.

P_{rad}: It stands for as an antenna radiated power.

2.2.3 Gain

"Relationship between an intensity in a particular direction and that which would be obtained if antenna-absorbed power were to be radiate isotopically" is how an antenna's gain is described in the definition above. When multiplied by four, it equals the antenna's ability to accept power [24]:

$$G = \frac{4\pi U(\theta,\emptyset)}{P_{in}(isotropic\ losess\ source)} \tag{2.3}$$

Unless otherwise specified, the power gain is typically in use in a direction of greatest radiation. A total input power by total radiated power (Prad) has been based on a total input power (p_{in}) by

$$p_{rad} = e_{cd} p_{in} \tag{2.4}$$

The relationship between gain and directivity

$$G(\theta,\emptyset) = e.D(\theta,\emptyset) \tag{2.5}$$

Where:

G: Gain of an antenna.

e: Efficiency [25].

2.2.4 Input Impedance

The relationship between the voltage at each electrode of the antenna and the current flowing through it is known as the impedance of the antenna. There are options for transmission cables operating at both low and high frequencies. According to the theory behind antennas, in order for the antenna to transmit, it needs to have its "impedance matched" to the transmission line. If the resistance of the antenna is not properly matched, the antenna will not emit any radiation. The resistance that is present at the terminals of the antenna is referred to as its antenna's input impedance.

Antenna ZA is described in terms of:

$$Z_A = R_A + jX_A \tag{2.6}$$

where RA stands for an antenna resistance in ohms and XA stands for an antenna reactance in ohms.

The radiation resistance can be stated by

$$Za = \ R_r + R_L + jX_a \tag{2.7}$$

Radiation resistance (rr) and loss resistance (rl) are two distinct measures of the same property. The only way for a substance to develop the ability to withstand radiation is for it to be subjected to actual power. When a lossless antenna is utilized, a rise in the radiation resistance also results in a rise in the input resistance. Another illustration of input impedance is the connection between voltage and current at its connections, in addition to the connection between the correct electric and magnetic fields at a particular location. One method for determining the input resistance involves employing an analogy circuit model of the antenna. The resistance of an antenna can be affected in a variety of ways, including by its shape, the way it is excited, and the frequency at which it operates. As an alternative to the more traditional empirical method, it is now feasible to compute the impedance of a broad variety of complex geometrical structures by making use of computational electromagnetic techniques [26].

2.3 EFFICIENCY

An antenna's power efficiency can be determined in one of two ways: the first is to examine the amount of power that it radiates and then evaluate that value in relation to the overall amount of power that it receives. Using this formula, you can calculate the efficiency of the antenna if you already have the values for the radiation resistance Rr and the loss resistance RL.

$$\eta_a = \frac{\text{power radited by antenna}}{\text{power input to the antenna}} = \frac{I^2 R_r}{I^2\,(R_r+R_l)} = \frac{R_r}{R_r+R_L} \tag{2.8}$$

The letter I represent the flow of current through the antenna terminals. By multiplying η_a by 100, one can get a percentage of antenna efficiency for the system [27].

2.4 RETURN LOSS (SLL)

When the load is mismatched, the entire power is not supplied to a load, and this phenomenon is referred to as a return of power. Return loss is an accurate and convenient method for calculating input and output signals. The measurement of return loss is considered to be of the utmost significance in antenna and cable networks (rl). These measurements provide the supervisor with insight into the system's fitness and whether or not it complies with the standards. During testing, potentially hazardous flaws could be discovered if they are not detected early enough. When antennas are not well-matched, there is an increase in the refraction of radio-frequency (RF) energy that is not available for transmission and is instead compressed in the transmitter [28].

2.5 BANDWIDTH

An antenna's bandwidth refers to the frequency range it is capable of transmitting or receiving energy over. If you want to know how well an antenna performs throughout a wide spectrum of frequencies, you can look up its broadband antenna performance. Broadband can also refer to the frequency range in which a certain antenna's features can be used.

2.6 MICROSTRIP ANTENNA (MA)

Microstrip patch antennas, also known as MPAs, are a form of planar antenna that has been the subject of a significant amount of investigation and innovation over the course of the past forty years. In recent years, there has been a rise in the number of wireless communication systems used for military and industrial purposes that make use of them, and antenna designers frequently opt for them. The technology of printed circuits can be used for more than just circuit components and transmission lines; it can also be applied to the radiation sources of an electrical system. It was decided to come up with a microstrip patch antenna concept. On one side of the MA, you'll typically find a "substrate" that has a particular thickness and is completely metalized on one of its outsides. On the other side of the MA, you'll find a metal "patch." Typically, the "substrate," which corresponds to the letter (d), has a powdery consistency. Even though this is the most typical shape, a unique appearance can be accomplished by applying just a small metal piece to the front surface of the item, as shown in Figure 2.4. This will allow the item to stand out from the crowd. On this subject alone, there are literally thousands of academic articles and a handful of books. There is a collection of reviews, articles, books, and chapters contained within the references [29][44].

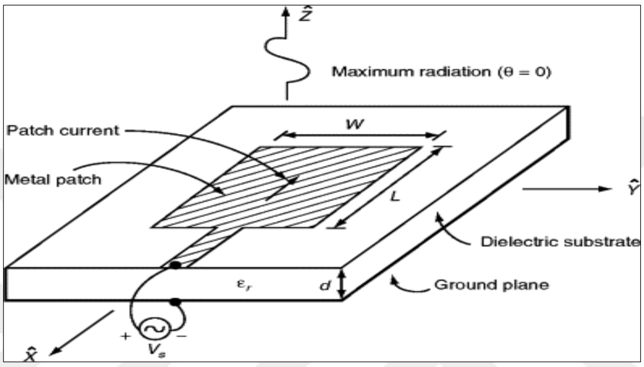

Figure 2.4: The Structure of MA [29][44].

2.7 MICROSTRIP LINE FEED

The microstrip patch is physically connected to the conducting microstrip feed line, which enables an efficient passage of electrical current. Because of the broad variety of diameters, the feed line and the microstrip patch are frequently used in conjunction with one another. Putting it together and putting it together is a piece of cake. Figure 2.6 provides a visual representation of microstrip line loading. In a microstrip patch antenna, a transmitting patch is located on one side of a dielectric substrate, and a ground plane is located on the other side [4][5]. Microstrip antennas are superior to conventional ones in terms of performance. This is due to the fact that they are superior in terms of size, weight, and volume, as well as the ease with which they can be manufactured using printed circuit technology. Because of the increasing demand for smaller and more discrete antennas in personal and mobile communications, there has been an increase in the use of microstrip patch antennas. This demand has led to the increased adoption of these antennas. Microstrip patch antennas can be utilized in a diverse selection of contexts. In spite of the many advantages it offers, there are a number of disadvantages associated with it as well. Some of the issues include high Q values, poor scan performance, and spurious input radiation [45]. This is just a sampling of the issues.

2.7.1 Microstrip Line Feed

As can be seen in Figure 2.5, one of the feeding methods involves a connection of an electrical conductor that is made immediately to the edge of the microstrip patch. It is feasible to etch the feed on the same substrate as the patch because the conducting strip is smaller than the patch itself. As can be seen in Figure 2.6, there is no requirement for an additional matching device because the patch already has an inset cut that corresponds to the resistance of the feed line.

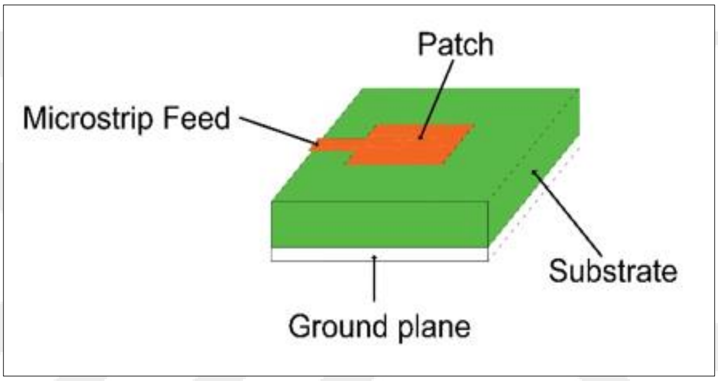

Figure 2.5: Microstrip Line Feed [45].

2.7.2 Co-axial Feed

Instead of a planar feeding methodology, this technique employs the use of a z coaxial cable to supply power to the patch. As shown in Figure 2.7, the dielectric allows for a metal contact to be established between the inner conductor of the coaxial connector and the patch, while the connector's external conductor can be connected to a ground plane. This probe is positioned precisely in front of an antenna that has an input resistance of 50 ohms so that we can use it as a point of reference. This feed mechanism is an alternative worth considering because it is straightforward to construct and releases only a negligible amount of radiation. When coupled with Ground Plane Connection [46], on the other hand, this presents a significant disadvantage.

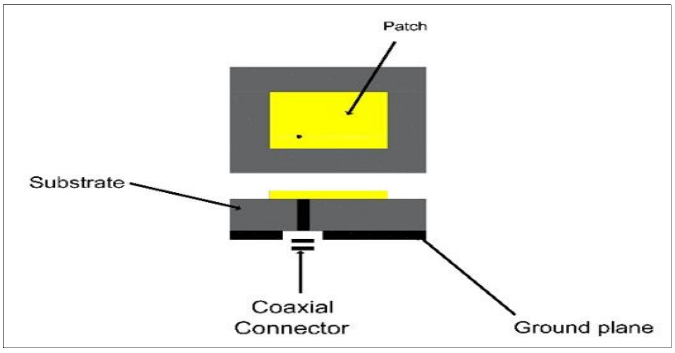

Figure 2.6: Co-axial Feed Line [46].

2.7.3 Aperture Coupled Feed

For the aperture feed method to work, the antenna dielectric substrate and the feed dielectric substrate must be used Figure 2.8. A ground plane with a centre slit separates the dielectric substrates. The antenna substrate is covered with a red metal patch see Figure 2.8. Antenna dielectric is located on the other side of antenna dielectric, which is where the ground plane is located. Insulation can be achieved by placing dielectric and feeder lines on the other side of ground plane. Aperture feeds are needed to achieve polarization purity that is impossible with regular feed methods. An antenna fed by an aperture has a greater range of frequencies. To save money, it is useful in situations where we don't want to run cables across layers. In order for this feed to function, a vast number of separate layers must be created.

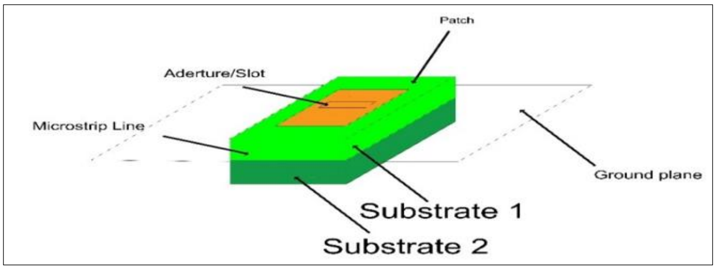

Figure 2.7: Aperture Coupled Feeding Method [47].

2.7.4 Proximity Coupled Feed

In contrast, the development of this nutrition mechanism is a challenging endeavour to undertake. Both types of insulating substrates are utilized in this method. Between the two dielectrics, it is possible to make out the microstrip patch that is located on the upper dielectric substrate as well as the input line [47]. It provides the greatest possible bandwidth while simultaneously lowering the quantity of radiation that it emits.

Figure 2.9 illustrates the proximity-linked data that is being used.

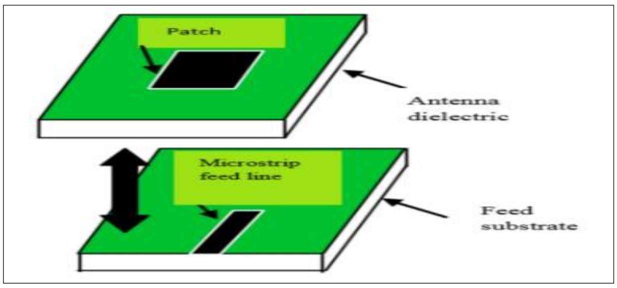

Figure 2.8: Proximity Coupled Feed [47].

Table 2.1: MSA Feeding Approaches are Compared.

S	characteristics	Line feed	Co-axial feed	Aperture coupled	Proximity feed
1	Spurious radiation	higher	higher	less	smallest
2	reliability	better	poor	good	good
3	fabrication	easy	Soldering needed	Alignment needed	Alignment needed
4	bandwidth	2-5 %	2-5 %	12-15 %	8-10 %

3. METHODS OF ANALYSIS

The microstrip antenna has been studied and examined by a number of researchers, each utilizing a different methodology. The full-wave, transmission line, and cavity models are among the most commonly used analytical models. When it comes to computing costs, a transmission line is the most cost-effective method. It can be used for any design and provides a substantial amount of information. Its findings aren't always precise, and it can be difficult to obtain enough evidence for the pairing to work. These are the qualities of models using the full-wave technique, according to published evidence: extreme flexibility; high precision; limitless or restricted displays; and the ability to tackle single, self-assertively produced, and stacked components; as well as coupling. Acknowledging their complexity and the fact that they often yield less physical knowledge than simpler models [48].

3.1 TRANSMISSION LINE MODE

The transmission line model is the most straightforward one, but it also has the lowest accuracy and the least amount of flexibility. Each of the L-radiating narrow slots is separated from the next one by a length that is denoted by the letter L. The amount of electromagnetic energy that can be transmitted through a slot in a rectangular microstrip antenna is determined by the slot's width and height measurements. The ZC transmission line model portrays the antenna as two slots that are separated by a low-impedance ZC transmission line running the length of the L. Utilizing this technique, one is able to determine the input performance of a rectangular patch antenna. The trapezoidal patch is the only pattern that can be used with this particular antenna. No other receiver makes use of it at all. This particular variant is utilized solely in rectangular patch antennas; it is not utilized in any other patch layouts. This illustration illustrates a microstrip antenna by using two slots, each of which has dimensions that are w, h, and L. Transmission lines of length L are placed between each pair of adjacent spaces. A non-homogeneous line of two dielectrics, most frequently the substrate and air, is used in the process of fabricating microstrip, which is a type of strip.

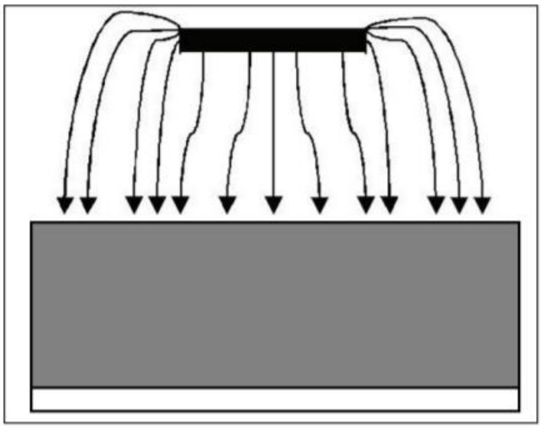

Figure 3.1: Electric Field Lines [48].

As can be seen in Figure 3.1, the vast majority of the electric field lines are embedded within the substrate, with only a select few emitting energies into the environment outside of the substrate. Because of the disparity in phase velocities between the air and the substrate, this transmission line is unable to sustain a pure Transverse-Electrical Magnetic (TEM) mode of transmission. In this particular situation, transmission in the quasi-TEM mode would be given top priority. In order to take into consideration fringes and wave propagation, it is necessary to calculate an effective dielectric constant, which is denoted by reff. According to what is seen in Figure 3.2, the fringing fields that are located around the patch's perimeter aren't confined to the dielectric substrate; rather, they are distributed throughout the air that is located around the patch, resulting in a mathematical formula for εε_reff that is smaller than ε r. [49].

$$\varepsilon_{reff} = \frac{\varepsilon_{r+1}}{2} + \frac{\varepsilon_{r_1}}{2}\left[1 + 12\frac{h}{w}\right]^{-1/2} \tag{3.1}$$

Were,

$\varepsilon_{\_reff}$ = Effective dielectric constant.

ε_r = Dielectric constant for a substrate.

h = dielectric substrate height.

W = Width for the patch.

Fig. 3.2 depicts a rectangular-shaped patch antenna supported by a substrate of depth h (L * W) (3.2). The x-axis characterizes length, y-axis signifies width, and the z-axis signifies height in the coordinate system arrangement.

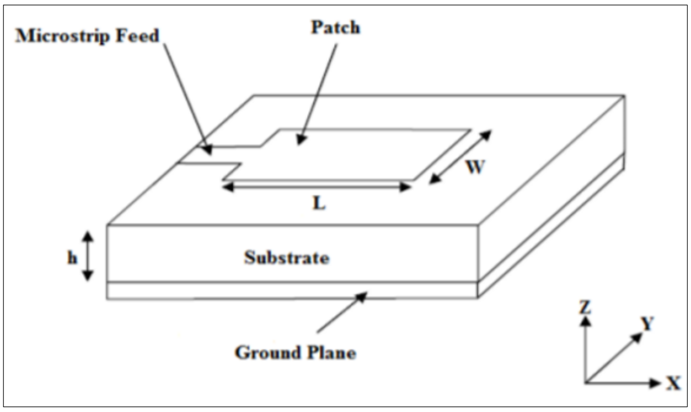

Figure 3.2: Microstrip Patch Antenna [49].

As displayed in Figures 3.3 and 3.4, a microstrip patch antenna has dual slots that are parted by an open-circuited and transmission line at both ends. As a result of having two open ends, a current has been small, but a voltage is large. When evaluated with respect to a ground, the electric field can be divided into tangential and normal components [50].

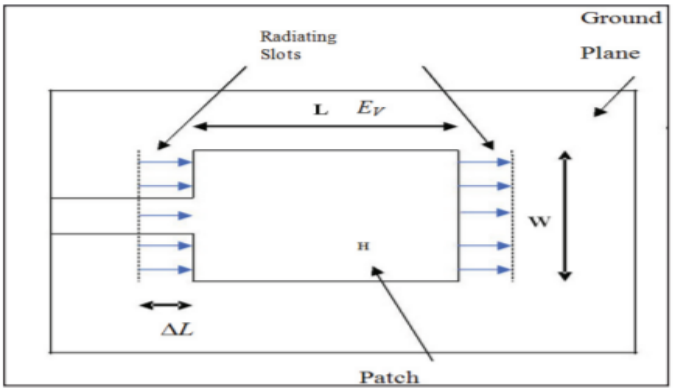

Figure 3.3: Antenna Top View [50].

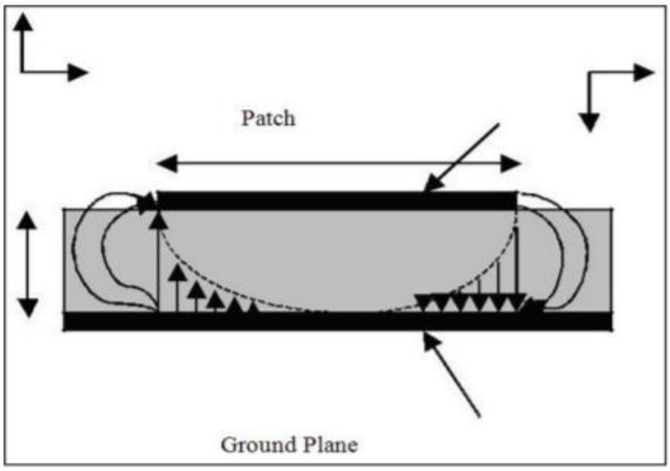

Figure 3.4: Antenna Side View [50].

An antenna's normal components of the electric field are usually in opposing directions at both ends of the antenna's breadth, which is compatible with the fact that they are often opposite in direction. As a result, they will neglect each other out in a broadside direction when a patch dimension is 1/2. An example of this is shown in Figure 3.3, which shows that the generated electric fields will have tangential component components that are in phase. Coordinate your efforts to produce the widest possible ray path normal to the building's surface. From now on, we'll refer to the antenna's two outside edges as its transmitting apertures. At a distance of two, the apertures each have the same energy in phase. The half-space along the railing is where they'll start.

$$\Delta L = 0.412h \frac{(\varepsilon_{reff}+0.3)\left[\frac{w}{h}+0.264\right]}{(\varepsilon_{reff}-0.258)\left[\frac{w}{h}+0.8\right]} \tag{3.2}$$

An effective length for a patch L_{eff} becomes L_{eff} $=L + 2\Delta L$ for specified resonant frequency fr, an effective length will be:

$$L_{eff} = \frac{c}{2fr\sqrt{\varepsilon_{reff}}} \tag{3.3}$$

$$f_r = \frac{c}{2\sqrt{\varepsilon_{reff}}}\left[\left(\frac{m}{l}\right)^2 + \left(\frac{n}{w}\right)^2\right]^{\frac{1}{2}} \tag{3.4}$$

Here, m and n stand for modes along L and W correspondingly designed for efficient radiation, a width W can be specified by [51-52]:

$$w = \frac{c}{2fr\sqrt{\frac{\llbracket(\varepsilon\rrbracket_r + 1)}{2}}} \tag{3.5}$$

3.2.1 Cavity Model

Indeed, a transmission line model described in a preceding paragraph has several fundamental problems, despite how simple it seems. For rectangular patches, it is especially useful because it doesn't take into account field fluctuations at the radiating boundaries. Because of these shortcomings, the cavity model could perhaps be adopted. An overview of this model can be found here.

The inside of the dielectric substrate is depicted in this model as a hollow, with two electric walls around it for thin substrates: (h). This area is only limited by patch metallization and ground plane due to the substrate's thinness, which creates a z-directed electric and transverse magnetic field with components Hx and Hy. The patch's regular behavior is for the inner region to exhibit little z-direction fluctuation. This observation has two electric barriers: one at top and bottom sides.

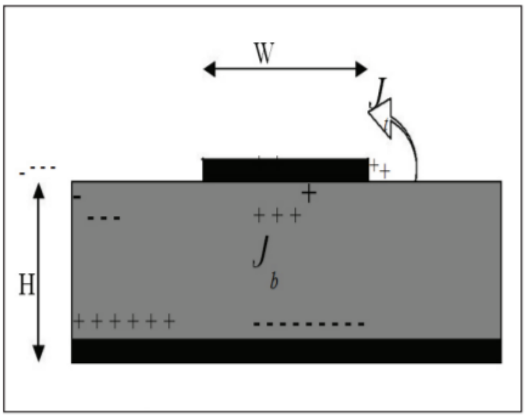

Figure 3.5: The Microstrip Patch's Charge Distribution and Current Density Creation [51][52].

An example of this is depicted in Fig. 3.5. Charge distribution can be visible on both of higher and minor surfaces of the patch's microstrip when electricity is supplied to the patch. These two mechanisms are used to regulate the distribution of charge. Patch and ground plane are attracted to one another to keep patch's charge concentration at the bottom. For whatever reason, some charges go from the patch's lower layer to its upper layer because they repel each other. Charge mobility allows these flows to travel on both the top and bottom surfaces. Cathode models promote attractive processes because of their moderate height-to-width ratio, which means that the bulk of the charge and current is deposited below their surfaces. The height-to-width ratio must be reduced and the current patch must shrink in order to sustain current flow on the upper surface [53]. Wireless technology has been an integral measure of our regular lives, from satellites in space to smartphones in our pockets. Because of this, it was created in an effort to provide better wireless technology services in a more user-friendly manner. In today's unpredictable energy supply climate, wireless energy may be a feasible alternative to gas and oil, which have variable prices. A wide range of research and projects are focused on energy harvesting technology with the goal of enhancing techniques for powering electrical and electronic equipment. It's possible to design a system that can collect energy from an enclosed room or public area, even if most of the radiation from electronic equipment is harmless.

3.2.2 Full Wave Analysis

A finite-wave solution, a finite difference time-domain method, in addition to a finite-difference approach are the most commonly used approaches for full-wave analysis. Full-wave analysis has a slew of unique features: With the finest solution accuracy in the business, you can rest assured using this software. Multilayer geometries and varied feeding methods can be used to manufacture microstrip pieces of any shape. It offers solutions that are data-dense in terms of comprehensiveness. has to do with coupling, loss of conductivity/dielectricity, and impacts on space waves. The effects of surface-wave radiation. To reduce the computing burden of full wave approaches, many adopt numerical methods [54].

3.2.3 Impedance Matching

Most technological fields, including communications and electronics, are becoming increasingly interested in impedance matching research. When termination is done appropriately, signal integrity is maintained and data throughput is increased. An impedance mismatch boundary in a radio frequency network returns power to the source. In order to attain the best feasible return loss, efficiency, and gain performance criteria, impedance matching becomes increasingly critical in an antenna design process. Instead of reshaping an antenna's shape, impedance matching can be used to quickly and easily fine-tune the antenna frequency range. An antenna's bandwidth can be increased by using impedance matching circuits to introduce extra resonances into the system. We use the 50-ohm characteristic impedance of most microwave sources and conduits to match antenna impedance [55]. Because of the importance of the rectifying circuit, RF energy harvesting research has received numerous awards and accolades. An RF-DC rectifying circuit is used to convert incoming antenna RF signals (AC type) into a DC output. A major problem is figuring out how to get DC voltage from low RF power inputs. There are two basic kinds of rectifier circuits investigated: diode-based and transistor-based. To build transistor-based rectifier circuits, diode effects are employed. In a rectifying circuit, the diode is the most important part. The efficiency of the rectifying circuit is described in Equation 3.6. For example, the PDC (PDC) is described by Equation [2], as a function of the power available at its input (PRF).

$$\mu = \frac{P_{DC}}{P_{RF}} \tag{3.6}$$

3.3 WIRELESS POWER TRANSMISSION SYSTEMS

Figure 3.5 depicts the block diagram for wireless power transfer, which consists of three fundamentally useful squares. It is necessary to convert power to microwaves in the principal square (DC to AC). After the antenna in the transmitter transmits the RF energy, it is sent over an electromagnetic link. The RF signal is transmitted to the receiver, which converts the RF power to direct current (DC) using a rectifier circuit. The effectiveness of the RF to DC conversion is influenced by the rectifier circuit utilized.. From now on, efficiency will be referred to as the ratio of input power (Pin) to output power (Pout) (Pin). Mathematically, a wireless power transmission system's overall efficiency (η) can be determined by dividing its DC output power at its reception end by its DC or AC input power at its transmitter end. $\eta all=\eta t\cdot\eta c\cdot\eta r$ A system's overall efficiency is the sum of all the efficiency gains made along the way, from the DC source all the way through RF transmission and reception, to the RF-to-DC conversion. Where ηt is the efficiency of the transmitter, ηc is the efficiency of the receiver, and ηr is the efficiency of the rectennas' microwave-to-electric transformation (PCE) or RF-to-DC power conversion (PCE).

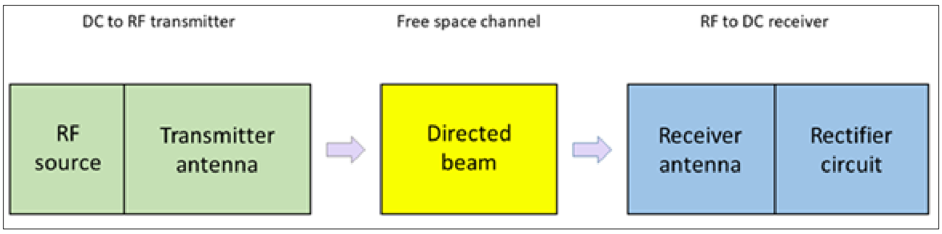

Figure 3.6: Depiction for WPT System [55].

The first term (ηt) is a sum of the magnetron effectiveness (ηmag) and an antenna efficiency (ηa). The RF source's efficiency is best described using the magnetron efficiency. The sender-side antenna efficiency shows the entire antenna efficiency, which takes the mismatch antenna factor into consideration. This means that the source generator is an appropriate device for transmitting power, as both magnetron effectiveness and the sender's efficiency are considered to be 100%. It is a ratio for received power to send power that determines a gathering efficiency (ηc). A sending antenna aperture must have an optimal power density distribution in order to maximize collecting efficiency. A design parameter (τ) known as Goubau's relation [56], states that if the impedance looking into the receiver is matched to the free space impedance, the collection efficiency must be exceptionally high.

$$\tau = \sqrt{A_r A_t}\ \lambda D \tag{3.7}$$

Calculating aperture dimensions can be done using Goubau's relation. Using Ar and At as a reference, we can say that the receiving and transmitting apertures' effective aperture areas are equal. The radiation's wavelength is given by the symbol. RF energy is converted into DC current by the receiver. Finding the correct diode is the most difficult part of picking the best DC to AC converter. This standard rectenna layout is shown in Figure 3.6. Wireless energy can be collected using antennas connected to rectification circuits via filters and a matching c.c.t. If you use an LPF before and after the rectifying circuit, your results will be more accurate. When the rectifying diode is in operation, high harmonic frequencies are generated, which can be separated and matched to the antenna with the rectifier circuit to obtain a higher AC to DC PCE with an LPF at the beginning and end of the rectifying antenna. Diodes are the heart and soul of the c.c.t. rectifier. Rectenna output terminal load term Figure 3.5 for DC voltage detection [57].

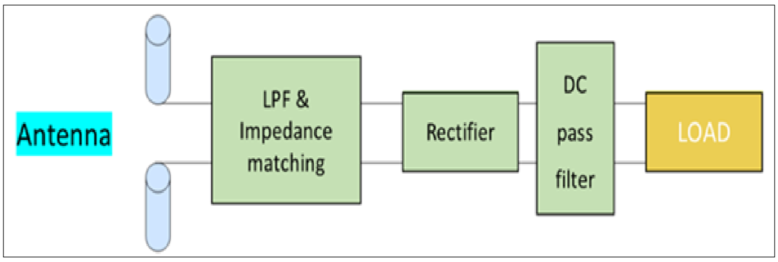

Figure 3.7: Rectenna Block Diagram [57].

3.4 EARLY EXPERIMENTS WITH WPT

The discovery by Hertz and Tesla that electromagnetic waves might be used to transport energy over vast distances led to the development of wireless power transmission (WPT). Low-frequency use of Earth's intrinsic electromagnetic resonance could be used to transmit electricity wirelessly. For future research of electromagnetic wave propagation, his idea will have a huge impact. The World Poker Tour (WPT) has gotten a lot of attention lately for a variety of reasons. There are numerous examples, including solar power transfer from space and remote vehicle propellers. Another way to gather energy is by harnessing stray electromagnetic fields. Wireless power transmission (WPT) was first proposed in the early 1900s. Electricity can be transferred wirelessly using WPT instead of cables. Charging a battery or operating a car with WPT requires significantly more power than doing it with radios or cell phones, which can only transport a small amount of energy. The elementary diagram of the WPT has depicted in Figure 3.7 The rectifying antenna, often known as the rectenna, is a critical component of any receiver [58].

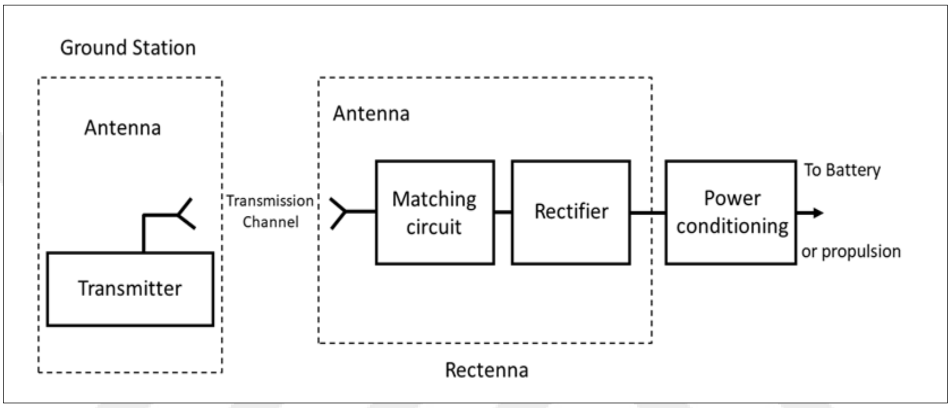

Figure 3.8: Generic WPT System Block Diagram [58].

3.5 RECTENNA CONCEPT

In 1963, R.H. George at Purdue University devised the microwave rectenna, but the Raytheon Company had the original idea. Brown created an aircraft using a 28-rectenna array during the 1960s. CBS Walter Cronkite News aired footage of helicopters hovering 60 feet above a microwave beam in October 1964. Figure 3.8 has images of the event, and Brown's book, "The History of Power Transmission by Radio Waves," provides a lot of detail [59].

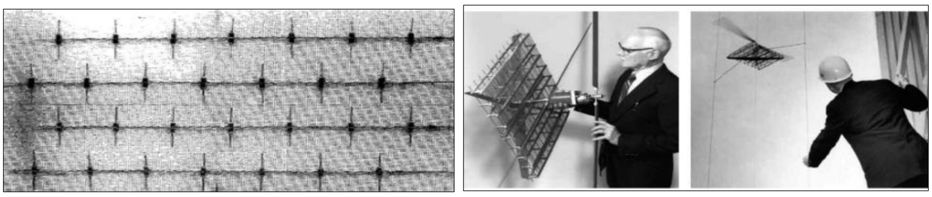

Figure 3.9: Images of the Event, and Brown's Book [59].

3.6 ENERGY HARVESTING

It's called "energy harvesting" when radio waves that are transmitted in the open air are converted into voltage. The price of electricity has risen significantly in recent days because of the high demand. Renewable energy sources are used to generate power. External energy harvesting is a technique for gathering and storing energy from the environment. Efficient energy harvesters rely on biomass and other natural resources. Use Using this strategy, which is also referred to as "power harvesting" or "energy scavenging," we can avoid having to buy new batteries for our little electronic devices, as well as the associated costs, inconveniences, and pollution that come with them. A few examples of probable sources include the wind, sun, thermoelectric, heel strike, vibration, temperature gradient, electromagnetic, pushbuttons, auditory, and radio frequency. Signal broadcasts from televisions, radios, wireless networks, and mobile phones use radio waves. It is possible to generate power using high-energy wireless transmissions [60]. Without the need of a physical media like wire or cable, electricity can be transferred from one location to another. The earliest theoretical understanding of wireless power transfer dates back to 1864, according to Maxwell. Toward the close of the 19th century, Nikola Tesla came into the picture. In the past, wire-free power was a laboratory experiment. A frequency of 150 was the key reason for their failure. Back then, high-frequency technology was a far cry from this. Wireless technologies have made it easier to communicate. Brown, William C., and colleagues. The rectifying antenna design used in the 1960s was dubbed "Rectenna" for this device. With a 7 WDC output, this rectenna's efficiency may be as high as 40%. In 1968, Brown's team conducted additional research into microwave power transfer. Industrial, scientific, and medical applications use microwave power transmission at frequencies as high as 5.8 GHz (ISM). For power transfers across great distances, the high efficiency of microwave power transfer is a big advantage. This means that we can test and enhance many various rectenna designs at 2.45 GHz [61]. An RF energy harvester is a device that converts electromagnetic energy from the environment into direct current (DC). Energy obtained from ambient RF sources is insignificant. A single antenna is insufficient because of the low incident power level. Several studies used a voltage multiplier rectifier to increase the gathered output.

It is a rectifier circuit that transforms the radio frequency (RF) signal from the antenna to direct current (DC). A Cockcroft-Walton voltage multiplier is the name given to the basic circuit of a Villard voltage doubler. Figure 1.10 displays an energy collecting system that is being tested. The RFDC conversion and load circuits are included. The RF input signal is harvested by an antenna with a matching circuit. This decreases the reflected current into the rectifier circuit through the matching circuit. A rectifier circuit transforms RF to DC and subsequently to the DC output load for various purposes. Numerous investigations have revealed the existence of this circuit. To create an AC signal, you may need to double the peak power of the alternating current's DC output [62].

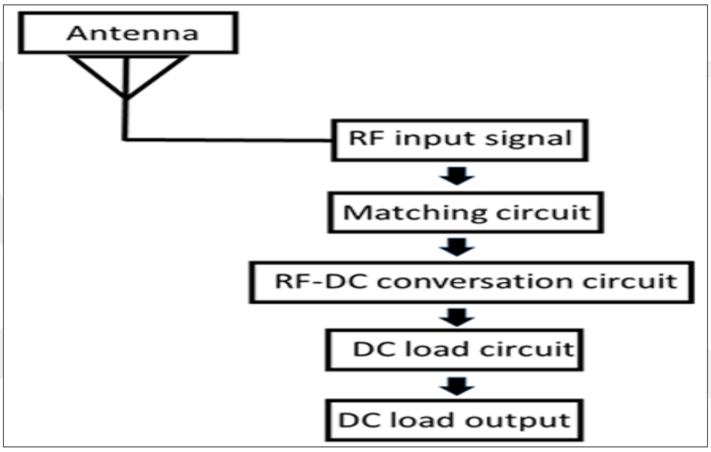

Figure 3.10: RF Energy Harvesting System [62].

4. SIMULATION AND MANUFACTURING PROCESS FOR MPA DESIGNS AND RECTIFIER CIRCUIT

To increase bandwidth, this study looks at several forms of energy-harvesting antennas. employing two distinct methods. Microstrip Patch Antenna (MPA) gain, return loss, bandwidth, and radiation pattern are addressed and demonstrated throughout this chapter.

4.1 DESIGN SPECIFICATIONS

Resonance Frequency (**fo**r): For a given use, the antenna's resonance frequency must be appropriate for that purpose. Our design incorporates UWB frequencies ranging from 3-13 GHz since they will be critical in meeting the demand for higher capacity in energy harvesting systems that are beginning to be commercially implemented all over the globe. The dielectric constant for a substrate (**εr**): The dielectric constants are generally in a range of $2.2 \leq \varepsilon r \leq 12$. An antenna's size may be reduced based on a substrate with a high dielectric constant [63].

a. Thickness for dielectric substrate (hs): For MPA to be employed in modern-day applications, it is important that an antenna isn' massive. Dielectric substrate height should be in the range of $0.003\lambda o \leq h \leq 0.05\lambda o$.
b. Conductor Thickness (ht): The default thickness for the copper which is 0.035 mm was used.
c. Loss Tangent (tanδ): The loss tangent affects the total size, radiation pattern, return loss and gain of the MPA.

4.2 PLAN AND DEVELOP A CPW-FED ULTRA-WIDEBAND ANTENNA FOR USE IN ENERGY HARVESTING

In this part, we'll go through the MPA's design, simulation, and findings. As a first step in developing an antenna design, CST software may be useful for estimating the S-parameters as well as other parameters like bandwidth and gain. The frequency response, a dielectric constant, then thickness for a dielectric substrate, the material type, and the input impedance are all important considerations in the design of an MPA.

Table 4.1 : The Parameters of MPA's Design.

Resonance frequency	$f_{\circ}$	3.1-10.6
Dielectric constant	ε_r	4.4
Height of substrate	h	1.5
Input impedance	z_{in}	50Ω
Material type	$FR-4$	

Figure 4.1 depicts the antenna's construction, which consists of CPW and specialized patch radiator slots that are divided into parallel and identical slots on either side [64]. When comparing printed slot antennas to microstrip antennas, printed slot antennas have several benefits. CPW employs active and passive components to modify and enhance existing single-wave circuits, and it can connect in either a parallel or serial configuration. A slot antenna has the same gain but more favourable characteristics such as wider bandwidth, greater dispersion, and reduced radiation loss. As an example of how the MPA looks in modelling software, see Figure 4.1-a. shows the measurements of the antenna in Figure 4.1b.

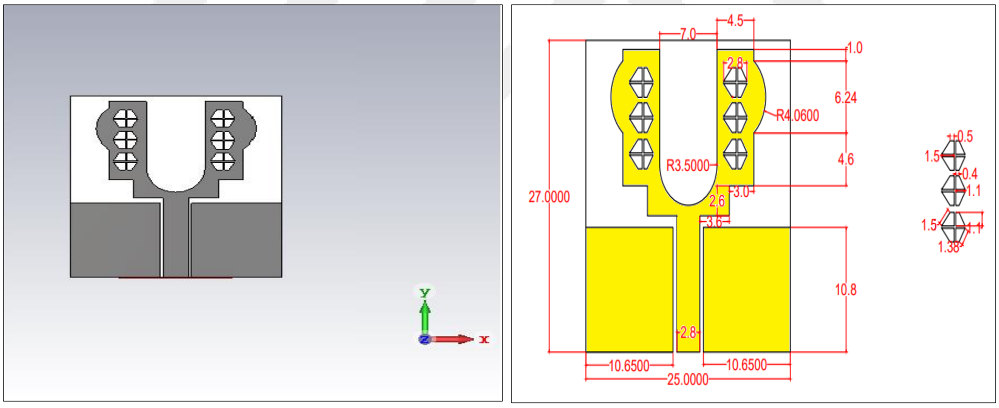

(a) (b)

Figure 4.1: a) MPA Inside Antenna Simulation Software, b) Dimensions of Antenna.

4.2.1 Simulation Results and Discussion

Many early antennas, such as the CPW antenna, were constructed using CST MWS software. A central frequency of 8.27 GHz, as shown in Fig. 2, has positive impacts at B.W=10 GHz. When the load is not present or when not all the power generated is usable for loading, -40dB input reflection is the easiest method for characterizing the input and output of the signal source. Figure 4.2 displays the outcomes of a scenario in which parameter S11 was set.

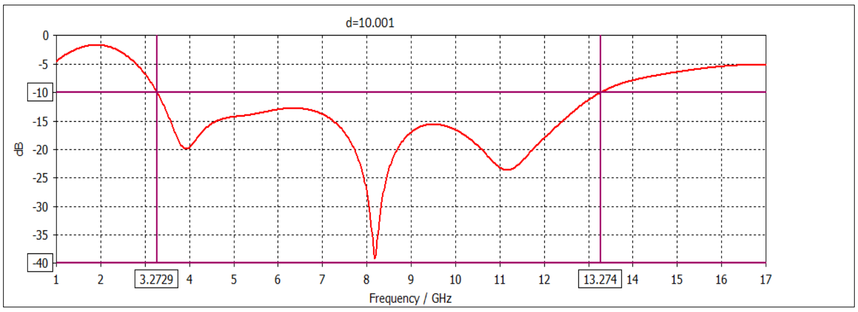

Figure 4.2: S11 for Projected UWB Antenna.

A look at the antenna's 3D radiation pattern in Figure 4.3 helps explain why it has the highest directivity gain of 3.71dBi at 8 GHz.

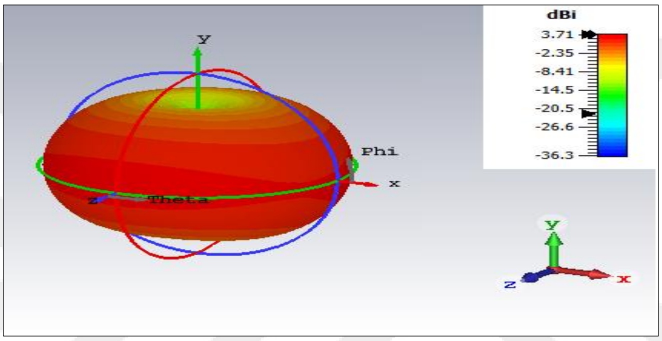

Figure 4.3: 3D Radiation Patterns @ 8GHz.

Antenna leading sections of UWB are depicted in Figure 4.3 with surface currents. Most of the power of the magnet is concentrated in the feeder, patch radiator's base, and borders with a magnetic strength of 5 A/m.

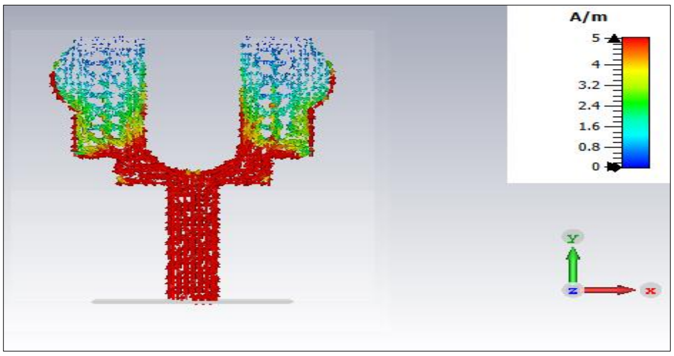

Figure 4.4: Surface Current Intensity Distribution.

The resistance of 3.27 to 13.27 GHz used to calculate the IEEE gain for ultra-wideband is displayed in Figure 4.5. Radiation far field in the x, y, and z planes as simulated by a computer is shown in Figure 4.6.

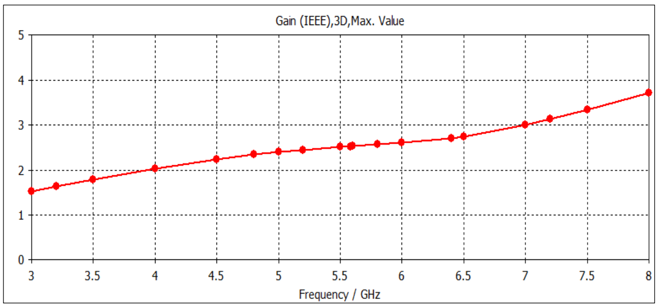

Figure 4.5: IEEE Gain for Projected Antenna.

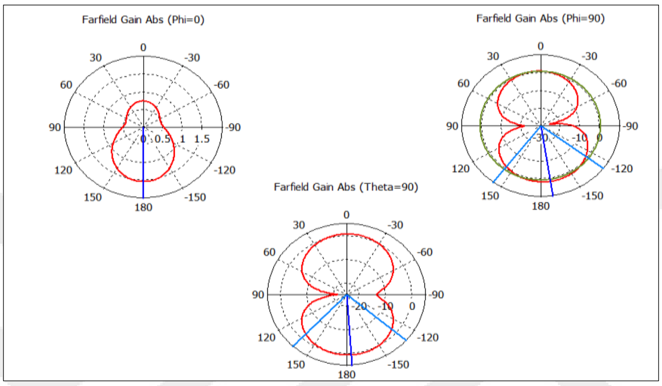

Figure 4.6: Radiation Patterns for Proposed Antenna (At 8 GHz).

Table 4.2: Comparison to the UWB Antennas that have been Reported.

Ref	Size (mm^2)	Bandwidth (GHz)
[65]	35x30	2.45 – 10.75
[66]	36x40	7.7- 11
[67]	30x35	7 – 10
[68]	50x50	5.82 – 15.07
[69]	40x35	3.1– 10.6
Proposed ntenna	**27x25**	**3.27– 13.27**

As a result of this study, the UWB and [65-69] antennas have been compared. As indicated in Table 4.1 I, the planned antenna size for this project is small enough to provide competitive bandwidth.

4.2.2 Second Design Miniaturized CPW UWB Antenna for Wireless Applications

The use of microstrip antennas is extremely prevalent in the field of wireless communication. Microstrip antennas offer a number of benefits thanks to their symmetrical and non-symmetrical planar shapes, as well as their cheap costs, lightweight construction, and ease of integration into arrays. The most efficient modes of communication are mobile phones and wireless transmission. Since it is able to rapidly conform to any shape that is presented to it, a microstrip antenna is a good choice for use in situations that call for a low-profile antenna. The capacity of a microstrip antenna to simultaneously function at a wide range of frequencies is the primary benefit that sets it apart from other types of antennas [70][71]. The use of microstrip antennas, which can be readily incorporated into a specific design, is strongly recommended. Even though a microstrip antenna can be designed using a number of different substrates, the frequency range of 1 to 100 GHz can only be applied to a single substrate at a moment [72]. A patch antenna comprises four sections (patch, substrate, ground, and feed). Microstrip antennas have a substrate that serves as an appropriate gate to sustain the patch and ground plane. This gate is located underneath the patch. If the antenna needs to be mounted on a structure that has a changeable shape, the antenna substrate or a flexible substrate made of materials that are flexible will need to be used. The medical field, the scientific community, and industry have all found numerous applications for flexible microstrip patches. Because the antennas need to be flexible and able to be bent, it is preferable to make the substrate layer as thin as feasible so that the antennas can have greater flexibility. When the substrate thickness is decreased, a microstrip patch antenna's frequency and gain both decrease as a direct result. It is necessary to increase the return loss, bandwidth, and strength of the antenna in order to get around this disadvantage. The antenna has a few disadvantages, the most notable of which are its low power and narrow bandwidth. In order to broaden the frequency range, patch antennas of a variety of geometries and dimensions were developed [73]. In order to satisfy the specifications for gain and bandwidth, modifications were also made to the ground plane and the patch. The widespread implementation of ground plane spaces has resulted in an increase in the MPA's bandwidth. When using this procedure, it is possible to generate a wide variety of frequencies [74][75]. CPW antennas have become increasingly popular due to the ultra-wideband characteristics that they offer. As a result, they are typically employed in applications that are both broadband and volume-limited. A representation in schematic form of the suggested design for the antenna, which is based on the Locked-Key topology, can be seen in Figure 4.7. This antenna was fabricated using a FR4 substrate that had a relative dielectric constant of 4.4 and a thickness of 1.5 millimetres. The antenna has an etched round feed slot at the beginning of its feed route. There is a striking resemblance between the 3 mm-wide feeder with equal-sized side openings and the keys for doors that have an impedance value of 50 ohm. The width of the foundation was 25 millimetres, the length was 27 millimetres, and the thickness was 1.5 millimetres. 0.35 millimetres was the distance that separated the transmission cable from the ground.

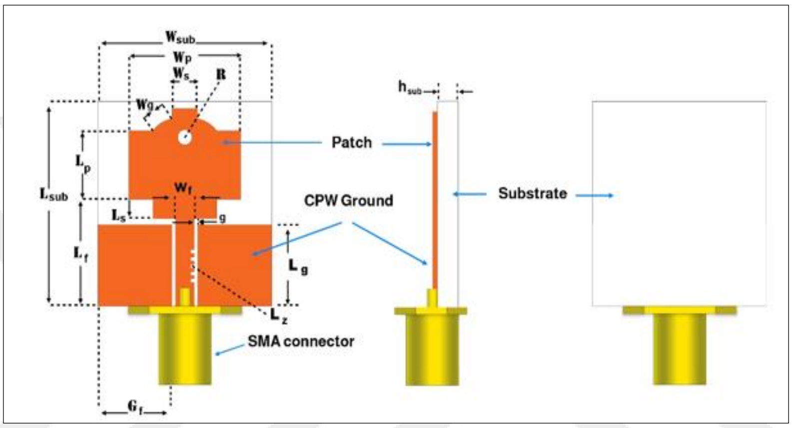

Figure 4.7: The Predicted Topology of the CPW Antenna, Which is Based on the Locked-Key Topology.

The construction and optimization processes for the proposed UWB antenna are illustrated in Figure 4.8. In accordance with the 'Trial and Error' methodology, the UWB frequency range of the projected antenna as well as the S11 parameter can be modified through a series of trial steps in order to achieve the desired band application. This is accomplished by resizing the external antenna dimensions in a manner that is inversely proportional to the fundamental frequency. Effective optimization predictors for the required UWB frequency range can be generated using factors such as slots, slits, the area of the microstrip patch, and the ground.

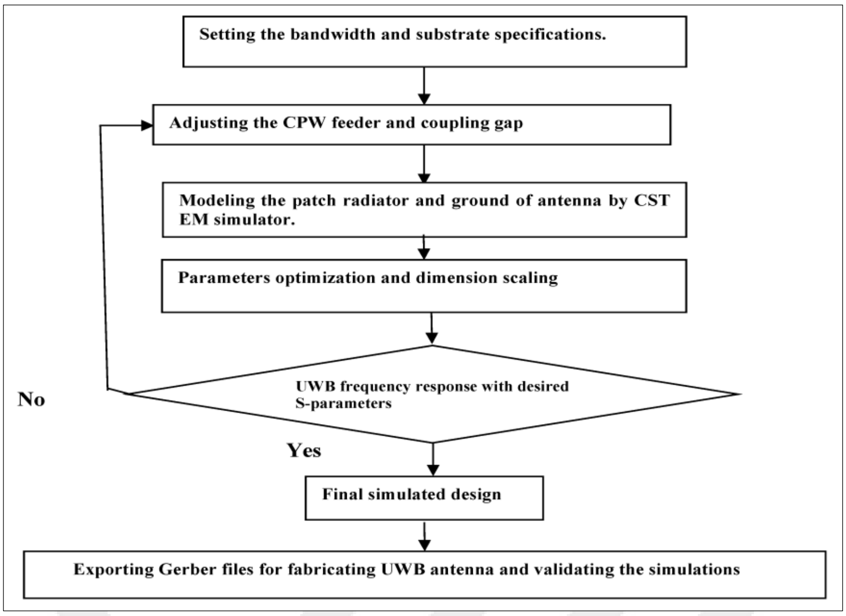

Figure 4.8: Procedural Steps for Design and Optimizing of S11 Responses of the UWB-CPW Antenna.

As a consequence of this, within the frequency range of 1 to 17 GHz, the influence of several different types of patch radiator on the input reflection performance of the CPW-fed antenna, which is depicted in Figure 4.9, has been investigated. For this purpose, the same FR4 substrate material and dimensions were utilized. Figure 4.10 reveals that the patch radiator in a, b, which does not have slots, possesses a dual band and notches, which can be seen in the frequency responses of Steps 1 and 2, with a modest difference in bandwidth. On the other hand, for Steps 3 and 4, the effectual UWB responses are apparent based on patch shape deformation with the applied circle slot; however, the antenna demonstrates a relatively higher bandwidth in Step 4 (Locked-Key topology) than in Step 3 due to the effect of circle slots and teeth slits. This is because of the combination of the two. As a result, we decided to proceed with this stage in order to manufacture and calibrate the UWB antenna we had envisioned.

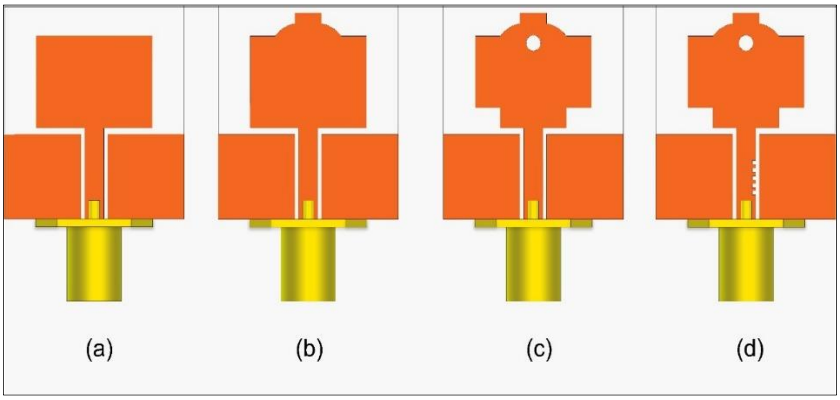

Figure 4.9: The Four Stages that Need to be Taken when Investigating Different Cases of the CPW-Fed Antenna Design.

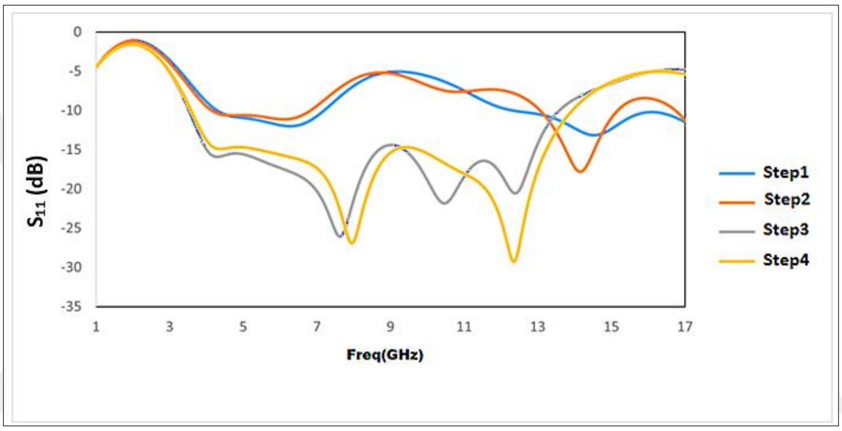

Figure 4.10: S11 Response for each Stage in the Proposed Design of the CPW-Fed Antenna.

In order to determine the fundamental lower frequency (FL) for the proposed UWB antenna, it was necessary to take into account the breadth and length of the substrate. The following equations were used to do this in a practical manner:

$$FL = \frac{0.53\ C}{Lsub\ \sqrt{\frac{\varepsilon r+1}{2}}} = \frac{0.49\ C}{Wsub\ \sqrt{\frac{\varepsilon r+1}{2}}} \tag{4.1}$$

where ε_r denotes the relative dielectric constant and c is the symbol for the speed of light in meters per second. At its lower frequencies of 3.581 GHz, the substrate size of the projected UWB antenna is approximately 0.53 λ_gby 0.49 λ_gin units of guided wavelength. This is the size of the projected antenna. In order to calculate the width and length of an antenna while making use of a slotted patch radiator, the following equations can be utilized:

$$Wsub = \frac{0.53C}{2\,FL}\sqrt{\frac{2}{\varepsilon_r + 1}} \tag{4.2}$$

$$Lsub = \frac{0.49C}{2FL}\sqrt{\frac{2}{\varepsilon_r + 1}} \tag{4.3}$$

Figure 4.11 is an illustration that was created with the help of a microwave office simulator that shows the RLC equivalent circuit for the intended UWB antenna as well as its input reflection response. The resistors and capacitors are connected in a configuration known as parallel. Altering the magnitudes of the resistors allows one to adjust the input reflection of a circuit model, while altering the magnitudes of the capacitors enables one to tailor the input reflection of a projected UWB antenna. Adjusting the impedance frequency range can be accomplished through the use of both the first and last inductors. The impedance bandwidth was measured to be anywhere between 3.4 and 14 GHz, which is strikingly similar to the planned bandwidth specification for the projected UWB antenna in this research.

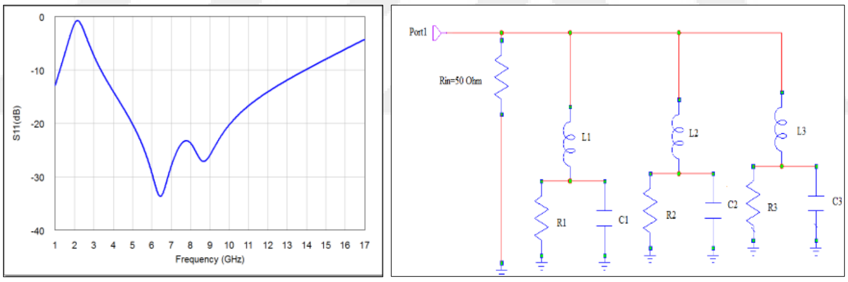

(a) (b)

Figure 4.11: a) An equivalent Circuit for Projected Antenna, and b) Its S11 Response.

4.2.2.1 Simulated results and discussion

The CST simulator, which is frequently utilized for the design of a wide variety of antennas, was employed in the process of developing and simulating the CPW-fed antenna. As can be seen in Figure 4.12, when the bandwidth (BW) was set to 10.354 GHz, the central frequency was 8.76 GHz, and the dispersion S11 parameter was considered to be satisfactory.

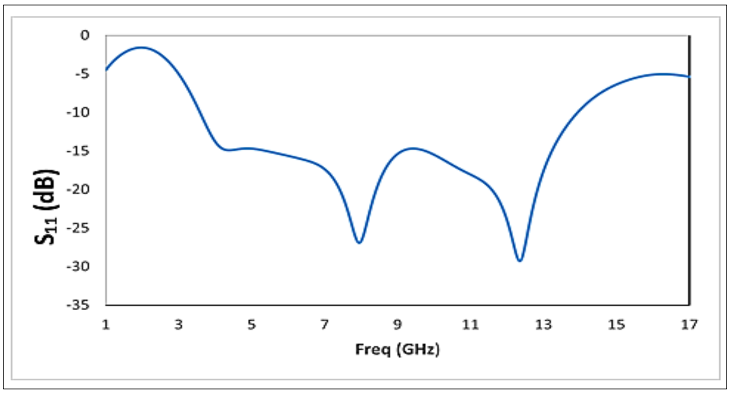

Figure 4.12: S11 for the Anticipated UWB Antenna.

The suggested ultra-wideband (UWB) antenna has a maximum gain of 3.02 dBi at a resonant frequency of 8 GHz and has a maximum gain of 3.72 dBi at a resonant frequency of 12.2 GHz, as shown in Figures 4.13 and Figure 4.14, respectively.

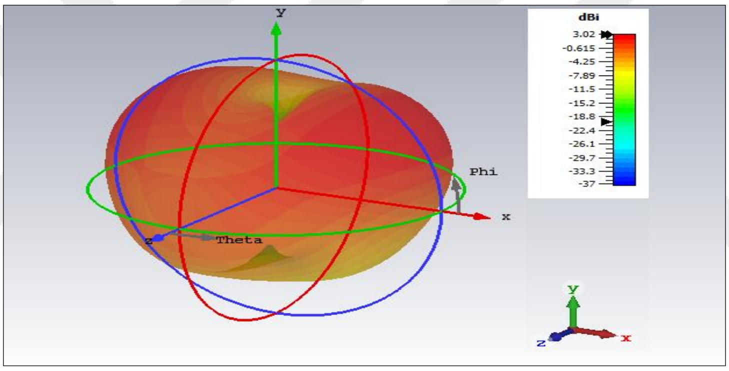

Figure 4.13: 3D Radiation Pattern at 8 GHz.

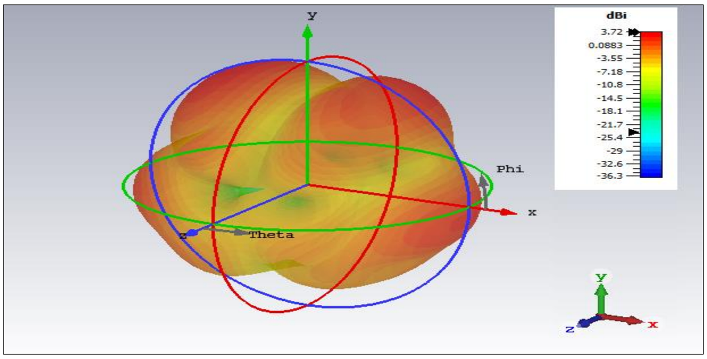

Figure 4.14: 3D Radiation Pattern at 12.2 GHz.

Figure 4.15 illustrates the surface current distribution in the different sections of the designed UWB antenna at frequencies of 3.58, 8.76, and 14 GHz. The highest magnetic strength was measured at 69.5 A/m across all of the resonant frequencies, and the most effective regions were found in the feeder and at the base of the patch radiator.

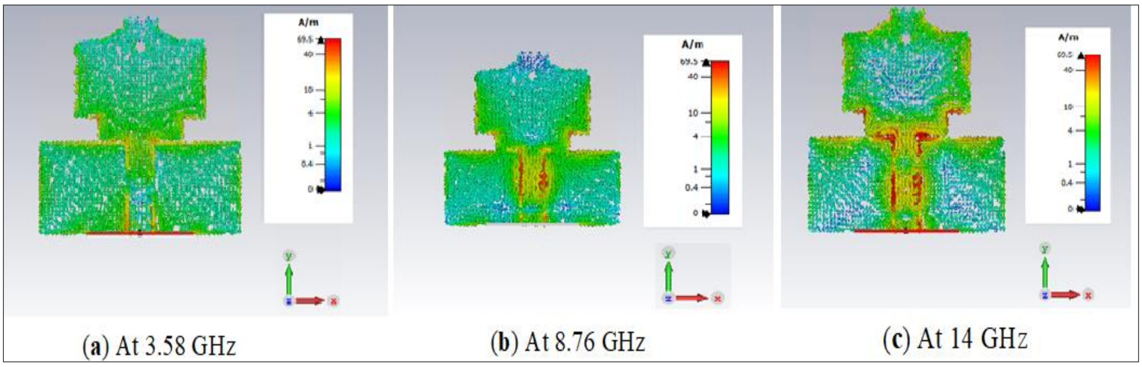

Figure 4.15: Current Intensity Distribution at a) 3.57 GHz, b) 8.76 GHz, and c) 14 GHz.

Within the frequency range of 1–17 GHz of the predicted UWB antenna, the gain value for UWB is demonstrated in Figure 4.16. In general, the gain of an antenna will improve as the operating frequency of the antenna increases. This did not happen completely, as can be seen in Figure 4.17, because efficiency, and not gain, determines the relationship between frequency and directivity. Gain, on the other hand, is determined by the amount of energy gained. The primary contributors to a decrease in efficiency are improper impedance matching between the feedline and the antenna, losses caused by conductors, and losses caused by dielectrics. It seems that one of the parameters that is used to determine losses is undergoing some kind of shift. Side lobes do develop and cause a loss of directivity in an antenna when the wavelength of the antenna is nearly equal to or larger than the wavelength of the signal being received. The results of the simulation of the far-field radiation pattern for the projected antenna at the specified frequencies are illustrated in Figure 4.18, which provides a polar plot of the radiation pattern in three planes at 3.581, 8, and 14 GHz. At these frequencies, the suggested antenna has shown evidence of sensible radiation pattern characteristics, with behaviors that are for the most part symmetrical. Comparing the total power radiated by the antenna to the total power obtained from the generator is one way to determine how efficient an antenna is at transmitting and receiving radiofrequency (RF) signals. This efficiency can be measured in part by an antenna's ability to compare the total power radiated by the antenna to the total power obtained from the generator. In actual use, an antenna's only target when its radiation efficiency is at its greatest is the empty space surrounding the antenna itself. The majority of the incoming power is lost due to losses in the antenna, such as metal conduction, dielectric, and magnetic losses, when radiation efficiency is low. This happens when an antenna has poor performance. As a result, Figure 4.18 presents an illustration of the effectiveness of radiation. Within the range of frequencies covered by the UWB spectrum, the highest radiation efficiency was greater than 82%.

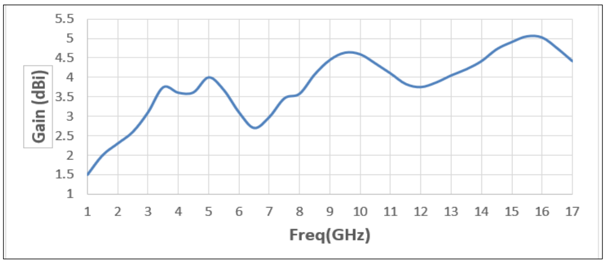

Figure 4.16: A gain for Proposed Antenna.

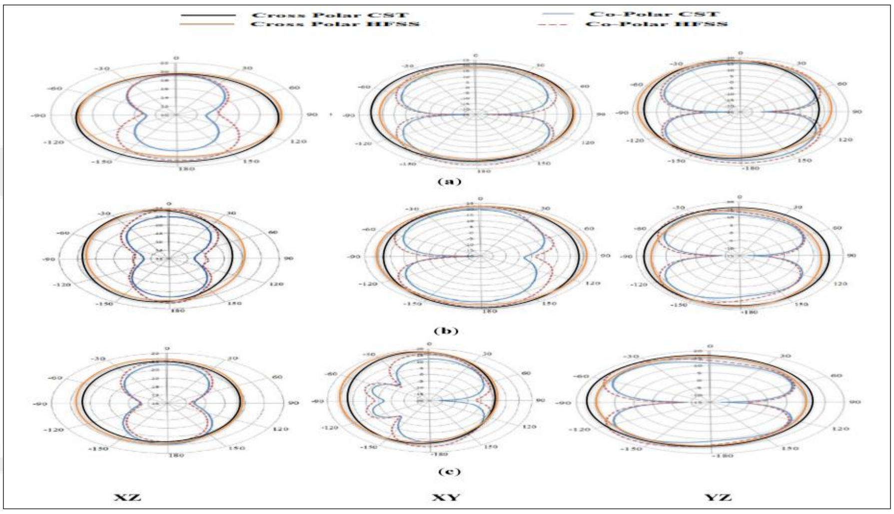

Figure 4.17: 2D Radiation Patterns of the Projected Antenna at a) 3.581, b) 8 GHz, and c) 14 GHz.

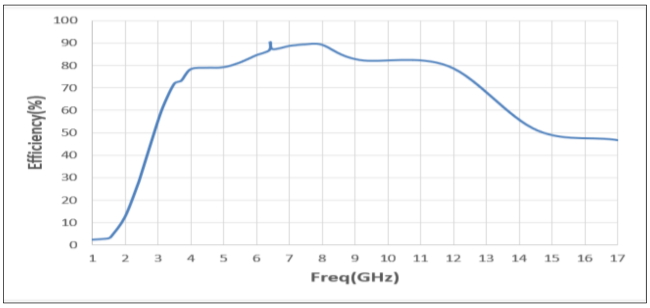

Figure 4.18: Radiation Efficiency for the Proposed Antenna.

4.2.2.2 Designing rectifier circuit for the second design

After the simulation of the antenna has been finished, CST MWS will construct and replicate a rectifier circuit. This circuit will first rectify the signal that was received through the antenna, and it will then supply power to the load. A low-voltage signal can also be amplified or converted with the assistance of boost or buck converters. In addition, a boost or buck converter might be utilized in this scenario if the signal has a low voltage. This design makes use of a voltage double as a rectifier circuit to change the alternating current (AC) signal that is received from the antenna into direct current (DC) output voltage. This type of circuit is referred to as a full-wave bridge circuit because it provides voltage for both the positive and negative cycles of the wave. We can get rid of undesirable harmonic frequencies by matching the impedance of the antenna with the input impedance of the rectifier, which is "50." This can be accomplished by using two stubs. Altering the dimensions (length and width) of both stubs in order to achieve the best return loss and match 2.45 GHz is the method that is used to carry out this matching procedure [76]. The maximum amount of power can be transferred between the antenna and the rectifier circuit as long as they are correctly matched to one another. To improve the multiplier circuit's efficiency while maintaining a low degree of power consumption, stub element matching is one strategy that has been considered.

4.2.2.3 Simulation and consequences for antenna and rectifier circuit

Because it is more difficult to design an LPF, the Stubs strategy was selected as an alternative. This is because the Stubs approach simplifies the circuit while also reducing the complexity of the circuit. The finished CST MWS antenna simulation is shown in Figure 4.19 and return loss is shown in Figures 4.20. It’s showed a low-pass filter representation of the data. Schottky diodes are perfect for the implementation of rectifier circuits because they have a low voltage threshold (which translates to a low voltage drop across the diode terminals) and a lower junction capacitance than PN diodes. This low threshold enables a more efficient functioning at low power levels, and the increased maximum frequency is due to the low junction capacitance of the diode. Because of its ability to transition forward and reverse at high speeds, a typical Schottky diode with the model number SMS-7630-005LF was chosen. Impedance matching is made challenging by the nonlinear behavior of Schottky diodes in energy harvesting circuits. This is because the resistance "Rs" is connected in series with a variable junction resistance "Rj" and in parallel with a variable junction capacitance "Cj." As a consequence of this, Schottky diodes were chosen because they allow for rapid forward switching while consuming a minimal amount of received power [77].

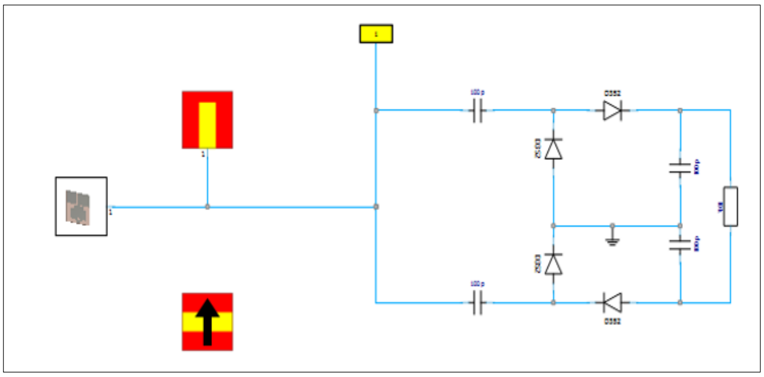

Figure 4.19: The Simulation for Antenna and Rectifier Circuit.

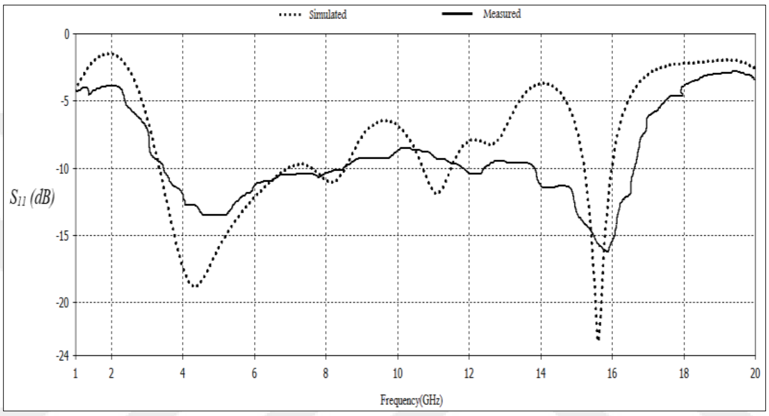

Figure 4.20: The Measured and Simulated S11 Responses of the Rectenna.

RF energy harvesting technologies hold great promise for the future of low-power electrical devices and sensor networks. In order to take up radio waves in the vicinity of 4.4 GHz, an ultra-wideband coplanar waveguide antenna was used, and the design was simulated with the help of the Antenna Magus software. CST MWS was used. This design makes heavy use of the Antenna Magus software in order to simplify the process of designing antennas. The use of a Schottky diode variant, SMS 7630-005LF, results in the antenna having a more compact form factor. Figure 4.21 illustrates the rectenna setup that will be used for the observations. The numbers of the output DC voltage are presented in Table 4.2. At 8 and 3 dBm of transmitter power, the dc voltages ranged from a peak of 1.65 V to a low of 0.5 V respectively.

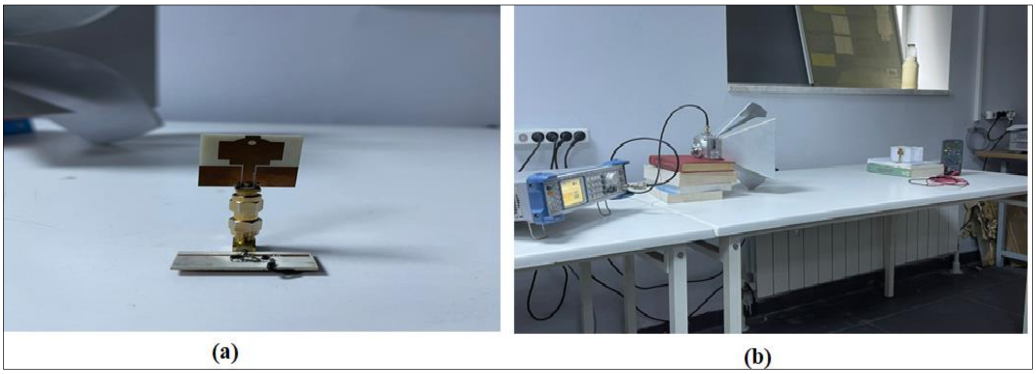

Figure 4.21: Rectenna Setup: a) UWB Antenna with Rectifier, and b) Rectenna Measurements.

Table 4.3: Transmitter Power and DC Output Voltage.

Transmitter Power (dBm)	Rectifier O/P Voltage (mv)
0	1.17
−1	1.14
−2	0.84
−3	0.50
−4	1.59
−5	0.89
−6	0.81
−7	1.19
−8	1.65
−9	1.48
−10	1.1

4.3 DESIGNING COMPACT UWB ANTENNA BASED ON FSSIR FEEDER

The proposed construction of the UWB antenna has been illustrated in Figure 4.21, and it has a dimension of (14 x 27.2) mm2 and a variety of slot sizes and configurations. FR-4 is used as the foundation in the construction of this antenna. It has a thickness of 1.5 mm and a permittivity of 4.3, and its measurement is the thickness. These substrate characteristics are available in the CST Microwave Studio application's material parameters interface. Copper is used to make both the decreased ground and the slotted patch, and both have a thickness of 0.035 millimeters. Feeders are segments of SIR that contain four phases and have their own unique name. Electrical lengths for four steps equal 3.75, with widths of 3, 1.5, 0.75, and 0.3525, and impedances of 50, 100, 200, and 400 Ohms respectively. Electrical lengths are measured in steps.

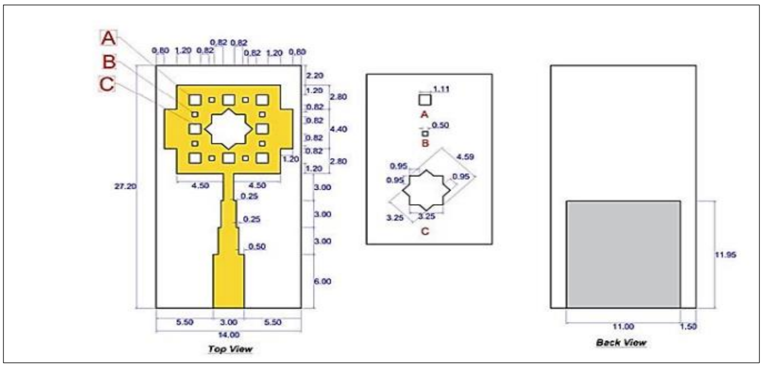

Figure 4.22: The Proposed UWB Antenna from the Top and the Back Sides.

4.3.1 Consequences and Discussion

The frequency range of 2.92–9.25 GHz is what the UWB antenna is designed to cover when it has the best possible complement. Figure 4.22 illustrates the input reflection reaction generated by the CST electromagnetic simulator. The values of the input reflection are 31, 30, and 32 dB, respectively, and they are found at resonant frequencies of 3.3, 5.75, and 7.1 GHz. The impedance bandwidth is approximately 6.33 GHz at a threshold of -10 dB.

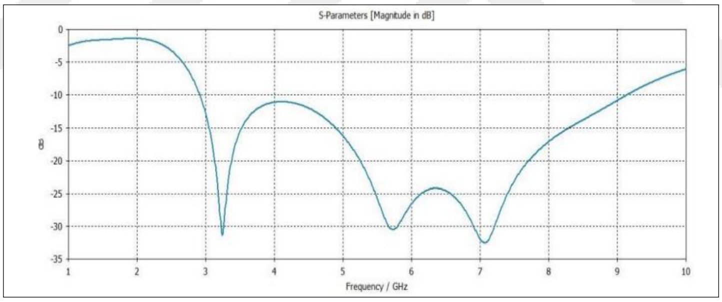

Figure 4.23: Input Reflection of the Proposed UWB Antenna.

At 3.2 GHz, the directivity gain for 3D radiation patterns is 1.68 dBi, while at 5.8 GHz it is 1.67 dBi, and at 7 GHz it is 1.56 dBi. These values are illustrated by Figure 4.23 a, b, and c. The characteristics of the substrate are what determine the gain of the antenna when it comes to microstrip antennas. The gain is directly proportionate to the thickness of a substrate, and it is inversely proportional to the distance between the two points. According to what is shown in Figure 4.24 the directivity improvement of 1.68 dB, 1.67 dB at 5.8 GHz, and 1.56 dB at 7 GHz is due to the 3D radiation patterns of the projected antenna.

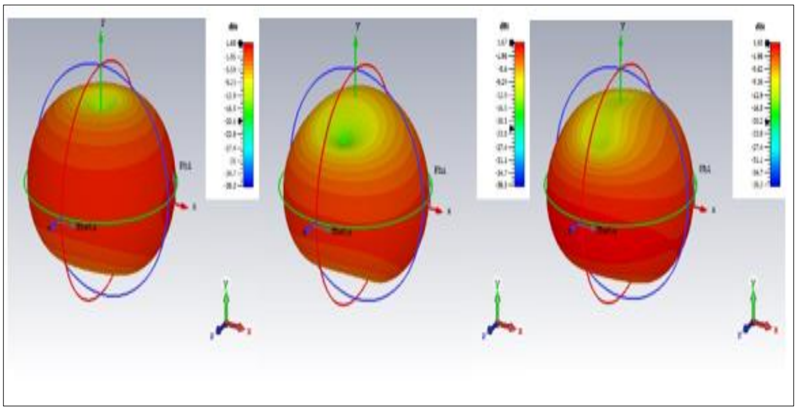

Figure 4.24: a).3D Radiation Pattern @ 3.2 GHz. b) 3D Radiation Pattern @ 5.8 GHz. c) 3D Radiation Pattern @ 7 GHz.

The simulated surface current distribution is shown in the regions where conductivity is present for the UWB-based antenna that is being planned. As seen in Figure 4.24, which represents effect regions based on the highest current intensity, the FSSIR feeder, slotted patch radiator bottom layer, and certain decreased ground plane margins all have a maximum current intensity of 5 A/m. This is the case for regions that are in effect based on the highest current intensity.

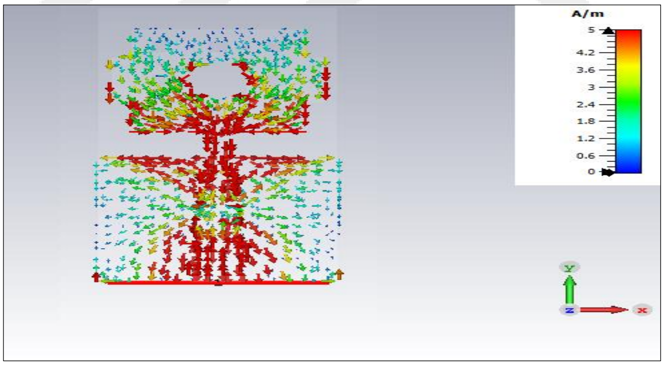

Figure 4.25: An Antenna's Surface Current Intensity is Distributed.

Using a UWB antenna with an impedance that falls anywhere between 3 and 7 GHz, it is feasible to achieve the IEEE gain that is depicted in Figure 4.26. Figure 4.27 presents the radiation fields that result from simulating far-distance patterns in three different planes: x-y, x-z, and y-z. Because they are perpendicular to the E plane and correspond to the H plane of a vertically polarized antenna, the x-y radiation patterns are examples of standard horizontal plane radiation patterns. Instead, the y-z plane and the E plane concur with one another in their presentation of the data. Given that this is the case, the y-z patterns are examples of radiation patterns in the vertical plane.

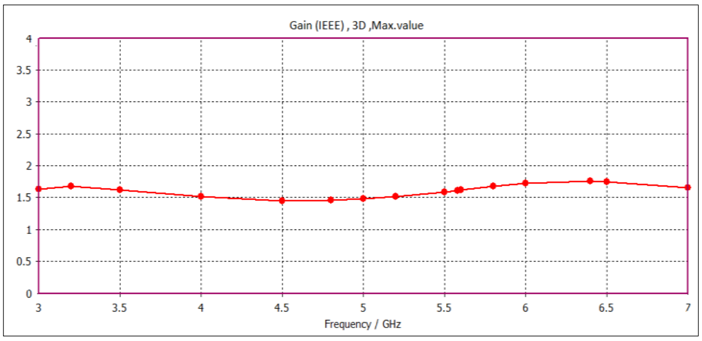

Figure 4.26: UWB Antenna Gain Based FSSIR Feeder.

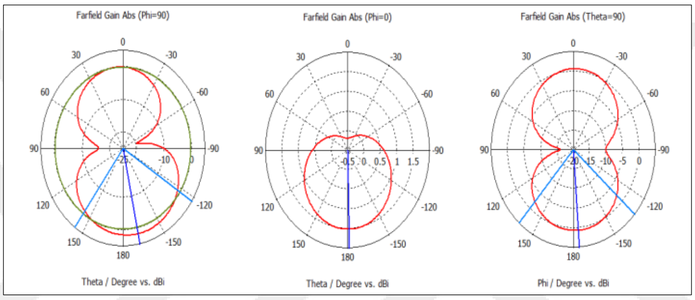

(a) 3.2GHz

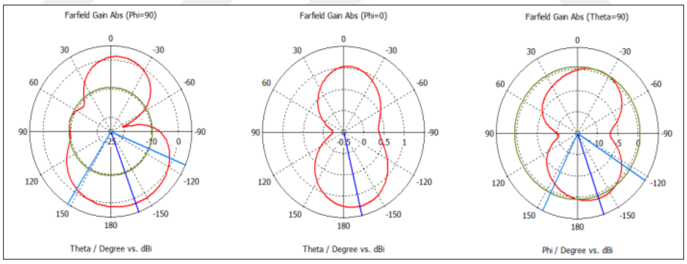

(b) 5.8GHz

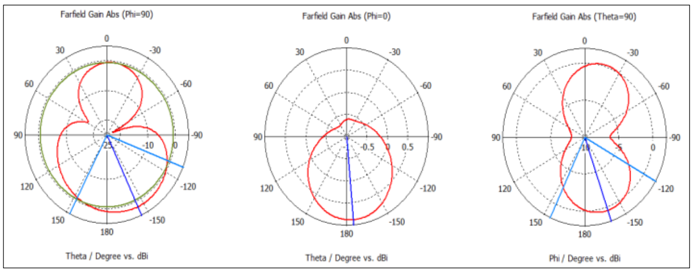

(c) 7 GHz

Figure 4.27: Radiation Patterns for Projected UWB antenna @ a) 3.2 GHz,b) 5.8GHz and c) 7GHz.

4.4 FABRICATION AND MEASUREMENT

4.4.1 Fabrication for Second Antenna

We constructed a prototype of the UWB antenna using an LPKF ProtoMat S63 and an Arduino. First, a model was constructed on FR4 epoxy substrate, and the feedline end was connected using a SMA coaxial connector see Figure 4.26 and Figure 4.27. As demonstrated in Figure 4.26, the Rohde & Schwarz®ZVB14 Vector Network Analyzer was utilized to test our prototype. As shown in Figure 4.27, the input reflection of the suggested CPW antenna can be simulated and measured to produce results that are consistent with one another. The S11 response, as well as the modest change in the UWB frequency band, can be identified in these results. The wide variation in S11 performance can be attributed to a number of different variables, such as the quality of the SMA connectors, the soldering process, the assembly process, and the dielectric substrate losses.

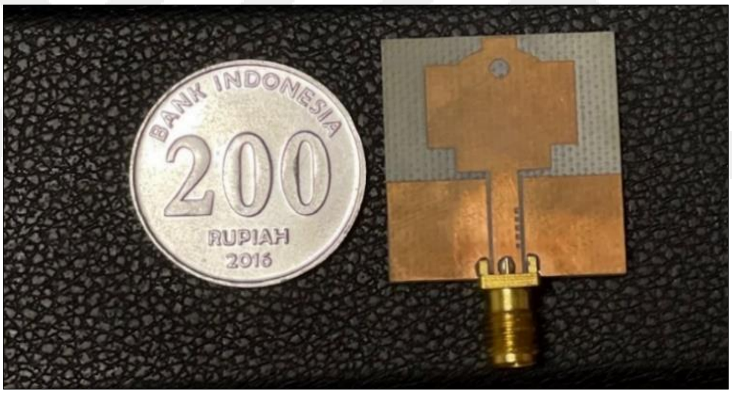

Figure 4.28: A fabricated CPW-Fed Antenna Prototype.

Figure 4.29: Antenna Measurement Operation.

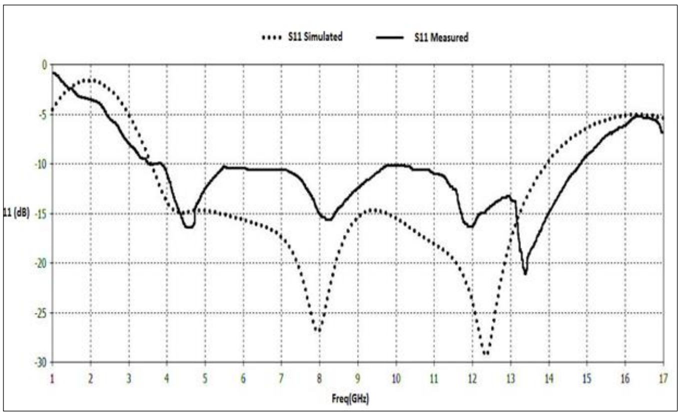

Figure 4.30: Input Reflection Responses for the CPW-Fed Antenna Based on Simulated and Measured Responses.

Using the antennas described in [78][79], a comparison was made between the UWB antennas discussed in this article and antennas that have previously been evaluated. As a result, it is planned to be as compact as is practically possible while still maintaining a bandwidth of useful impedance, as shown in Table 4.3.

Table 4.4: Comparative Magnitudes between the Reported UWB Antenna Configurations and the Designed UWB Antenna in this Study are Shown in this Graph.

Ref.	Max. Efficiency (%)	Max. Gain (dBi) within the Band	Dielectric Constant	Size (mm^3)	λ_g^2 at the Lower Frequency Band	Bandwidth Range (GHz)	Applications
[80]	83	3.18, 3.93	4.3	30 × 35 × 1.6	1.514917	7–9.9	UWB applications (X-band)
[81]	---	5.5	4.4	59.5 × 30 × 1.6	1.832615	5.85–6.6	Industrial Scientific and Medical Band applications.
[82]	88	6.08	4.4	36 × 42 × 1.6	0.91854	4.5–13.5	C and X band applications
[83]	--	3.5	4.4	47 × 47 × 1.6	0.26508	2–9.5	S and C band applications
[84]	40	--	2.2	27 × 33 × 0.787	0.14256	3–11 (with 5 notches)	UWB radiofrequency identification (RFID) is used for indoor localization
[85]	---	4	4.4	44 × 27 × 0.8	0.3425	3.1–10.6	UWB multiple-input and multiple-output (MIMO) applications

Table 4.3: Comparative Magnitudes between the Reported UWB Antenna Configurations and the Designed UWB Antenna in this Study are Shown in this Graph "Table Continued"

[86]	27	4.35	4.4	80 × 67 × 0.13	2.201352	3.7–10.3	Wearable antenna applications
[87]	85	8	4.4	50 × 44.4 × 0.15	3.452544	7.2–9.2	Wearable antenna applications
[88]	----	4.8	2.6	50 × 55 × 1.6	0.23567	2.07–2.83	Application of wideband and multiband frequency
[89]	73.4	3.7	2.2	100 × 50 × 0.78	0.056889	0.8–3.7	Energy harvesting
[90]	58	3	2.25	75.5 × 63.5 × 1.6	3.221004	6.1–7.7	Energy harvesting
[91]	60	4.55	3.5	32 × 28 × 2.5	0.014336	0.8–10	Low-Energy Applications
[92]	44.5	5.4	4.4	30 × 34.5 × 1.56	0.77625	5–6	Scalable RF Battery
[93]	52.	3	4.4	38 × 38 × 1.6	0.260878	2.454–2.45	Wi-Fi Energy Harvesting
[94]	87	7	4.4	50 × 40 × 1.6	0.0486	900 MHz–3 GHz 5.6 GHz–9.9 GHz	RF Energy Harvesting Applications
Proposed	82	4.7	4.4	27 × 25 × 1.5	0.259677	3.581–13.935	Energy harvesting

4.4.2 Fabrication and Measurements For uwb Antenna Based on fusser

LPKF machines have been used to create a prototype of the proposed UWB antenna. This prototype includes all design procedures and optimization based on the CST simulator. As can be seen in Figure 4.30, the opposite end of the feedline that was made out of FR4 resin substrate was connected to a SMA coaxial connection. Experiments with measurements that were performed with an Anritsu Vector Network Analyzer are illustrated in Figure 4.31. The simulated S11 result and the measured S11 result are identical, as can be seen in Figure 4.32. However, there are some tolerable differences that can be attributed to soldering, Cu losses, substrate losses, connecting cables, and the measuring surroundings.

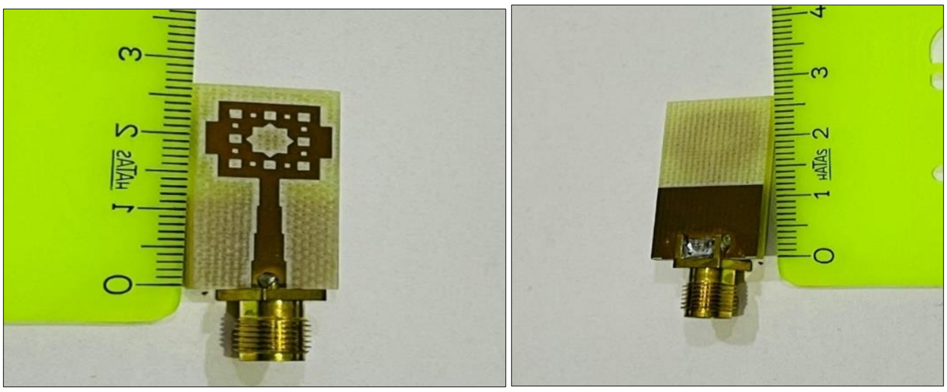

(a) (b)

Figure 4.31: Prototype Images of Projected UWB Antenna: (a) Top View and (b) Bottom View.

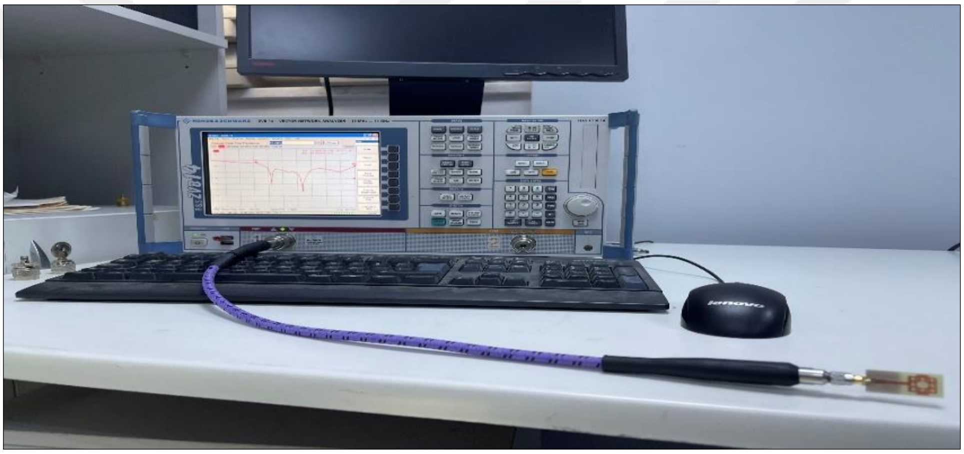

Figure 4.32: Antenna Measurement Operation.

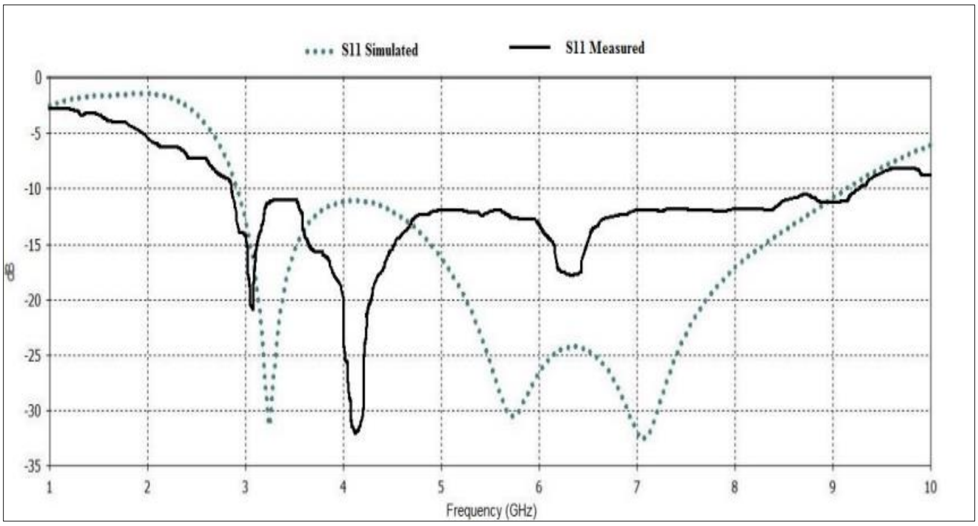

Figure 4.33: Measured S11 Response for the Projected UWB Antenna.

The UWB antenna described in this article has been contrasted with the antennas that were reported in [94][103]. As a consequence of this, the antenna that is discussed in this article is intended to have the smallest possible footprint while still preserving a workable impedance bandwidth, as can be seen in Table 4.4 In comparison to other antennas that are described in the literature, the antenna that was suggested for use in this investigation has very small dimensions, it is cost-effective, it has the highest bandwidth possible, and it is simple to manufacture.

Table 4.4: Magnitude Comparisons between the Various Reported Configurations of UWB Antennas and the Designed Configurations of UWB Antennas Used in this Research.

Ref.	Dielectric Constant	Size(mm^3)	Bandwidth Range (GHz)	**Applications**
[94]	4.3	30×35×1.6	7 – 9.9	UWB applications (X-band)
[95]	4.4	60x120x1.5	0.75-7.65	CR enabled wireless devices
[96]	2.2	63x56x0.34	28.5-27.4	5G applications
[97]	3.38	5x50x0.41	3-11.57	UWB/WiMAX applications
[98]	4.4	59.5×30×1.6	5.85-6.6	Industrial Scientific and Medical Band applications.
[99]	2.8	50x55x1.6	2.73- 2.83	Applications of wideband and multiband frequency.
[100]	4.9	50x40x1.6	1.62-2.7	Efficiency and Bandwidth Improvement
[101]	9.15	49x52x2.2	5.98-6.1	Applications for wireless and satellite communications.
[102]	4.4	50x44.4x0.15	7.2-9.2	Wearable applications.
[103]	4.4	60x80x1.6	7-8	C-band wireless communication.
Proposed	4.3	14x27.2	2.91-9.13	UWB applications

5. CONCLUSIONS

5.1 CONCLUSIONS

This research presents an ultra-compact CPW UWB antenna for use in today's wireless neighborhoods as a potential solution. Antennas with a Locked-Key topology were developed in order to circumvent the restrictions imposed by the substrate and the architecture of UWB antennas that existed before this breakthrough. During the printing procedure, a substrate that possessed a dielectric constant of 4.4 was utilized. In this investigation, we utilized feeders that possessed impedances of 50 ohm. The S11 scattering calculation came to the conclusion that the UWB bandwidth should be 10.354 GHz. The discoveries that were predicted by S11 are extremely similar to the observations that have been made. There have been descriptions in the past of UWB antennas that were much bigger and had much more restricted bandwidths. The design of the antenna that is presented in this article has the potential to be useful in upcoming energy harvesting applications. so, this cutting-edge technology for collecting RF energy can be useful for low-power devices like electrical and sensor network infrastructure. The antenna is connected to the amplifier that is used for the antenna in this configuration so that the rectification circuit can use it. A cpw antenna is utilized in order to acquire radio signals as well. The antenna design process, which was based on CST MWS and Antenna Magus, was sped up with the help of the software known as Antenna Magus. The SMS 7630-005LF type antenna with Schottky diode can be found in a small case, which contributes to the antenna's compactness. After putting the simulations through their paces, the findings. An antenna of this magnitude had an outstanding return loss of -30 dB, which was measured in decibels. A new compact UWB antenna with an FSSIR feeder was proposed in the second design in order to satisfy the requirements placed on wireless communities at the present time. This antenna, which is based on the FSSIR feeder, was designed with a slotted patch resonator and a decreased ground plane in order to circumvent the constraints imposed by the substrate and the UWB antenna design. The simulation of this antenna was also carried out using these elements. During the printing procedure, a substrate that had a dielectric constant of 4.4 was utilized as the base material. The feeder used impedances in the 50-ohm region for its operation. With the help of a simulated S11 scattering response, we were able to acquire UWB bandwidths ranging from 2.91 GHz to 9.13 GHz with satisfactory input reflections. The S11 simulations have produced predictions that are extremely similar to the actual effects that have been seen. According to the findings of recent research, this antenna is both more compact and effective than other UWB-based antennas currently on the market. These antennas are fabricated in a wide variety of unconventional designs, and the design modifications that were implemented to shrink their size and enhance their functionality are described in detail. This technique has the potential to improve our understanding of the performance of the patch antenna in a variety of settings. The findings of this research may be useful in improving the Reconned design for RF energy harvesting in the future.

This thesis will stimulate researchers in electromagnetic energy harvesting because it starts with an explanation and discussion of several ideas put forward with the goal of downsizing and improving bandwidth. Due to a particular characteristic, patch antennas can also be utilized in the construction of rectennas. Covid-19, which makes it difficult to build an open-lined resonator in the frequency range of 11.2 and 5.8 GHz, will be used in the design of the circuitry for the resonator, and its efficiency may be evaluated. This will make it more difficult to create an open-lined resonator. Additionally, the possibility of ultra-wideband rectification should not be discounted. In subsequent research, increasing the overall rectenna gain might require either an array approach or a substrate that is significantly more substantial. The effectiveness of the PCE as a whole is improved, as is its contribution to reducing wave mismatch and increasing antenna gain.

REFERENCES

[1] T. Rogalski, P. Flaszynski, P. Doerffer, and K. Doerffer, “Wind Turbines and Bridges,” 2022.

[2] N. M. Aljamali, A. H. Enad, and F. W. El-taei, “Engineering Design of Wireless Communications and Networks: Review Engineering Design of Wireless Communications and Networks: Review,” 2021.

[3] F. S. Alatallah, J. M. Imran, and A. A. Ahmed, “Design Microstrip Patch Antenna and Improved Radial Properties to Reach the Dual-Band Antenna Suitable for GPS and WLAN Applications,” J. Mech. Eng. Res. Dev., vol. 44, no. 8, pp. 151–157, 2021.

[4] M. Shakib, M. Moghavvemi and W. Mahadi, "Design of U-shaped feed structured antenna for ultrawideband application", Journal of Computational Electronics, vol. 15, no. 2, pp. 627-633, 2015.

[5] A. Abbas et al., "A Rectangular Notch-Band UWB Antenna with Controllable Notched Bandwidth and Centre Frequency", Sensors, vol. 20, no. 3, pp. 777, 2020.

[6] Pratik Chandgude. “Design of Microstrip UWB Antenna for Wireless Application.” International Journal of Engineering Research, pp.989–991, 2020.

[7] E. D. Hussein, N. Qasem, M. S. Jameel, M. Ilyas, and O. Bayat, “Performance optimization of microstrip patch antenna using frequency selective surfaces for 60 GHz,” in 2020 28th Signal Processing and Communications Applications Conference (SIU), 2020.

[8] N. Awad and M. Abdelazeez, "Multislot microstrip antenna for ultra-wide band applications", Journal of King Saud University - Engineering Sciences, vol. 30, no. 1, pp. 38-45, 2018.

[9] Kalamani, M., Krishnamoorthi, M., Valarmathi, R. S., Shalini, E., & Karthic, N. “Design of compact antenna for ultra-wide band applications.” International Journal of Engineering and Advanced Technology, pp.54– 57, 2018.

[10] S. Kundu, A. Chatterjee, S. Jana and S. Parui, "A Compact Umbrella Shaped UWB Antenna with Gain Augmentation Using Frequency Selective Surface", Radio engineering, vol. 27, no. 2, pp. 448-454, 2018.

[11] Al-Husseini, M., Ramadan, A., Tawk, Y., El-Hajj, A., & Kabalan, K. Y. “Design and ground plane optimization of a CPW-fed ultra-wideband antenna.” Turkish Journal of Electrical Engineering and Computer Sciences, pp.243–250, 2011.

[12] T. Shanmuganantham, K. Balamanikandan and S. Raghavan, "CPW-Fed Slot Antenna for Wideband Applications", International Journal of Antennas and Propagation, vol. 2008, pp. 1-4, 2008.

[13] R. Vivek, S. Sreenath, P. Vinesh and K. Vasudevan, "Coplanar Waveguide (Cpw)-Fed Compact Dual Band Antenna For 2.5/5.7 Ghz Applications", Progress in Electromagnetics Research M, vol. 74, pp. 51-59, 2018.

[14] L. Lazović, B. Jokanovic, V. Rubežić, and A. Jovanović, “Printed Ultrawideband Cardioid Monopole Antenna for Energy Harvesting Application,” 2019 14th Int. Conf. Adv. Technol. Syst. Serv. Telecommand. TELSIKS 2019 - Proc., pp. 134–137, 2019.

[15] M. Jenath Sathikbasha and V. Nagarajan, “DGS based multiband frequency reconfigurable antenna for wireless applications,” Proc. 2019 IEEE Int. Conf. Common. Signal Process. ICCSP 2019, pp. 908–912, 2019.

[16] A. J. A. Al-Gburi, I.B.M. Ibrahim, M.Y. Zain, and Z. Zakaria, “Compact Size and High Gain of CPW-Fed UWB Strawberry Artistic Shaped Printed Monopole Antennas Using FSS Single Layer Reflector,” IEEE Access, vol. 8, pp. 92697–92707, 2020.

[17] B. T. P. Madhav, J. Gogineni, H. Appana, J.P. Chennam, D.S.S. Thota, and P. Kotte, “Analysis of compact coplanar waveguide fed slot antenna with EBG structure,” Int. Conf. Signal Process. Commun. Eng.Assoc. with IEEE, pp. 219–225, 2015.

[18] Ahmad S, Ijaz U, Naseer S, Ghaffar A, Qasim MA, Abrar F, Parchin NO, See CH, Abd-Alhameed R. “A Jug-Shaped CPW-Fed Ultra-Wideband Printed Monopole Antenna for Wireless Communications Networks.” Applied Sciences. 2022.

[19] Al-Gburi AJA, Ibrahim IM, Zakaria Z, Abdulhameed MK, Saeidi T. “Enhancing Gain for UWB Antennas Using FSS: A Systematic Review.” Mathematics. 2021.

[20] Jamal, A., Bin, I., Zakaria, Z., Ahmad, B.H., Azwan, N. et al. “High Gain of UWB Planar Antenna Utilizing FSS Reflector for UWB Applications.” CMC-Computers, Materials & Continua, pp.1419–1436,2022.

[21] Benkhadda O, Ahmad S, Saih M, Chaji K, Reha A, Ghaffar A, Khan S, Alibakhshikenari M, Limiti E. “Compact Broadband Antenna with Vicsek Fractal Slots for WLAN and WiMAX Applications.” Applied Sciences. 2022.

[22] T. Varum, J. Caiado, and J. N. Matos, “Compact ultra-wideband series-feed microstrip antenna arrays for iot communications,” Appl. Sci., vol. 11, no. 14, 2021.

[23] S. D. Choudhary, G. Arora, S. Singh, and V. Shekher, “Microstrip patch antenna for GPS/WIMAX/WLAN applications,” Int. J. Recent Technol. Eng., vol. 8, no. 2, pp. 26–28, 2019.

[24] T. Peter, T. A. Rahman, S. W. Cheung, R. Nilavalan, H. F. Abutarboush, and A. Vilches, “A novel transparent UWB antenna for photovoltaic solar panel integration and RF energy harvesting,” IEEE Trans. Antennas Protag., vol. 62, no. 4, pp. 1844–1853, 2014.

[25] S. K. Terlapu, P. S. R. Chowdary, C. Jaya, V. V. S. S. Sameer Chakravarthy, and S. C. Sampath, “On the Design of Fractal UWB Wide-Slot Antenna with Notch Band Characteristics,” Lect. Notes Electr. Eng., vol. 471, pp. 907–912, 2018.

[26] M. S. Jameel, Y. S. Mezaal, D. C. Atilla, and E. D. Hussein, “A Compact Coplanar Waveguide Fed UWB Antenna for Energy Harvesting Applications,” 7th Int. Conf. Eng. Emerg. Technol. ICEET 2021, vol. 63, pp. 175–184, 2021.

[27] S. Kassim et al., “Flexible Co-Planar Waveguide (CPW)-Fed Y-Shaped Patch UWB Antenna for Off-Body Communication,” J. Phys. Conf. Ser., vol. 1464, no.1, 2020.

[28] M. A. Al-Janabi and S. K. Kayhan, “Flexible Vivaldi Antenna Based on a Fractal Design for Rf-Energy Harvesting,” Prog. Electromagnet. Res. M, vol. 97, pp. 177–188, 2020.

[29] M. Kgwadi, “Low-cost antennas and systems for next generation wireless communications,” pp. 1–128, 2017.

[30] A. A. Kishk, “Fundamentals of Antennas,”2014.

[31] I. Engineering, “Chapter 2 Fundamental Antenna Parameters.”

[32] Qin, Pei-Yuan, et al. "A pattern reconfigurable U-slot antenna and its applications in MIMO systems." *IEEE transactions on Antennas and Propagation* IOSR J. Appl. Phys., vol. 6, no. 3, pp. 24–38, 2014.

[33] C. Balanis, “Antenna Theory - Analysis and Design,” 2nd Ed., John Wiley and Sons.

[34] M. A. Al-Janabi and S. K. Kayhan, “Flexible Vivaldi Antenna Based on a Fractal Design for Rf-Energy Harvesting,” Prog. Electromagnet. Res. M, vol. 97, pp. 177–188, 2020.

[35] S. Karkare, K. Tewari, and E. Department, “Enhancing Return Loss of Rectangular Microstrip Antenna Using AMC Ground Plane,” Int. Res. J. Eng. Technol., vol. 2, no. 4, pp. 1045–1048, 2015.

[36] D. Gadhavi and T. Pansuriya, “2. 45 GHz Antenna Designs with Impedance Matching Network,” pp. 60, 2018.

[37] I. J. Bahl and P. Bhartia, “Microstrip Antennas,” Artech House, 1980.

[38] J. R. James, P. S. Hall and C. Wood, “Microstrip antenna theory and Design,” Peter Peregrinus, 1981.

[39] J. R. James and P. S. Hall (Editors), “Handbook of Microstrip Antennas,” Peter Peregrinus, 1989.

[40] D. M. Pozar, “Microstrip Antennas,” Proceedings of the IEEE, vol. 80, No. 1, pp. 79–91, 1992.

[41] Jean-Francois Zurcher and F. E. Gardiol, “Broadband Patch Antennas,” Artech House, 1995.

[42] K. F. Lee and W. Chen (Editors), “Advances in Microstrip and Printed Antennas,” Wiley Interscience, 1997.

[43] K. L. Wong, “Design of Nonplanar Microstrip Antennas and Transmission Lines,” Wiley Interscience, 1999.

[44] G. Garg, P. Bhartia, I. Bahl, A. Ittipiboon, “Microstrip Antenna Design Handbook,” Artech House. L. Wong, “Compact and Broadband Microstrip Antennas,” Wiley Interscience, 2002.

[45] K. L. Wong, “Planar Antennas for Wireless Communications,” Wiley Interscience, 2003.

[46] G. Kumar and K. P. Ray, “Broadband Microstrip Antennas,” Artech House, 2003.

[47] Z. N. Chen and M. Y. W. Chia, “Broadband Planar Antennas,” John Wiley & Sons, Ltd. 2006.

[48] K. F. Lee and K. M. Luk, “Microstrip Patch Antennas,” Imperial College Press, 2011.

[49] J. Huang, “Microstrip Antennas: Analysis, Design and Applications”, Chapter 4 in Modern Antenna Handbook, Edited by Constantine A. Balanis, John Wiley & Sons, Inc. 2008.

[50] J. Huang and D. M. Pozar, “Microstrip Arrays: Analysis, Design, and Applications”, Chapter 3 in Advances in Microstrip and Printed Antennas, K. F. Lee and W. Chen Editors, Wiley Interscience, 1997.

[51] K. F. Lee and K. F. Tong, “Microstrip Patch Antennas — Basic Characteristics and Some Recent Advances,” Proceedings of IEEE, vol. 100, no. 7, pp. 2169–2180, 2012.

[52] D. R. Jackson, “Microstrip Antennas”, Chapter 7 in Antenna Engineering Handbook, Fourth Edition, Edited by John L. Volakis, 2007.

[53] L. Shafai, “Wideband Microstrip Antennas”, Chapter 16 in Antenna Engineering Handbook, Fourth Edition, Edited by John L. Volakis, 2007.

[54] A. SB, A. Rufai, and A. M., “Review of Feeding Techniques for Microstrip Patch Antenna,” Int. J. Comput. Appl., vol. 178, no. 27, pp. 39–43, 2019.

[55] N. Kumar and N. Sharma, “The Various Feeding Techniques of Microstrip Patch Antenna Using HFSS,” Int. J. Electron. Common. Eng., vol. 6, no. 6, pp. 23–29, 2019.

[56] A. N. P. Arameters, “Microstrip Patch Antenna Parameters, Feeding Techniques and Shape of the Patch - A Survey,” vol. 6, no. 4, pp. 981–984, 2015.

[57] B. S. T. Al-moathni, “Energy Harvesting using Microstrip Patch Antennas,” 2019.

[58] Ashokrao, P. S., Hate, S. G., & Rakshit, S. M. “ Design of UWB Microstrip antenna with band-notch for interference avoidance.” International Journal, pp. 565-570.

[59] Suh Young-Ho and Chang Kai, "A novel dual frequency rectenna for high efficiency wireless power transmission at 2.45 and 5.8 GHz," in Microwave Symposium Digest, 2002 IEEE MTTS International, pp. 1297-1300 ,2002.

[60] T. Shanmuganantham, K. Balamanikandan, and S. Raghavan, “CPW-Fed Slot Antenna for Wideband Applications,” Int. J. Antennas Protag., vol. 2008, pp. 1–4, 2008.

[61] N. Muqarrab, M. I. Khattak, M. R. Zaffar, W. Shahjehan, and Z. Ullah, “Slotted Flexible UWB Antenna,” 2018.

[62] A. Al-Ahmadi and Y. S. H. Khraisat, “Bandwidth Enhancement of Microstrip Patch Antenna,” Appl. Phys. Res., vol. 11, no. 1, pp. 35, 2019.

[63] L. Tao et al., “Bandwidth Enhancement of Microstrip Patch Antenna Using Complementary Rhombus Resonator,” Wire. Common. Mob. Compute., vol. 2018, 2018.

[64] V. Bhanumathi and S. Swathi, "Bandwidth enhanced microstrip patch antenna for UWB applications," ICTACT Journal on Microelectronics, vol. 4, no. 4, pp. 669-675, 2019.

[65] K. A. Fante and M. T. Gemeda, “Broadband microstrip patch antenna at 28 GHz for 5G wireless applications,” Int. J. Electr. Comput. Eng., vol. 11, no. 3, pp. 2238–2244, pp.2238-2244,2021.

[66] M. P. Magalhães, “Design and analysis of an antenna array system for communication using high-altitude platforms,”2017,

[67] T. Shanmuganantham, K. Balamanikandan, and S. Raghavan, “CPW-Fed Slot Antenna for Wideband Applications,” Int. J. Antennas Protag., pp. 1–4, 2008.

[68] N. Muqarrab, M. I. Khattak, M. R. Zaffar, W. Shahjehan, and Z. Ullah, “Slotted Flexible UWB Antenna,” 2018.

[69] A. Kumar and M. Gupta, "Design, comparative study and analysis of CDMA for different modulation techniques", Egyptian Informatics Journal, vol. 16, no. 3, pp. 351-365, 2015.

[70] Q. M. Hamza, S. M. Nabil, and M. Hassan, “Novel CPW-fed UWB antenna for X-band applications,” vol. 4, no. 2, pp. 78–82, 2019.

[71] Pratik Chandgude, “Design of Microstrip UWB Antenna for Wireless Application”, International Journal of Engineering Research and, vol. 9, 2020.

[72] Benkhadda, O. Ahmad, S. Saih, M. Chaji, K. Reha, A. Ghaffar, A. Khan, S. Alibakhshikenari, M. Limiti, E. “Compact Broadband Antenna with Vicsek Fractal Slots for WLAN and WiMAX Applications. Sci. 2022.

[73] Anveshkumar, N. Gandhi, A.S. “A survey on microstrip antennas for portable wireless communication system applications.” In Proceedings of the 2017 International Conference on Advances in Computing, Communications and Informatics (ICACCI), Udupi, India, pp. 2156–2165,2017.

[74] Seker, C. Güneşer, M.T. “A single band antenna design for future millimeter wave wireless communication at 38 GHz.” Eur. J. Eng. Form. Sci, pp.34–38,2018.

[75] Khanna, P. Sharma, A. Singh, A.K. Kumar, A. “A novel approach for production challenges of flexible microstrip patch antenna.” Brill. Eng, pp.7–12,2019.

[76] Mondal, K. “Bandwidth and gain enhancement of microstrip antenna by frequency selective surface for WLAN,” WiMAX applications. Sadhana 2019.

[77] Al-Ahmadi, A. Khraisat, Y.S.H. “Bandwidth Enhancement of Microstrip Patch Antenna.” Appl. Phys. Res. 2019.

[78] Hamza, Q.M. Nabil, S.M. Hassan, M. “Novel CPW-fed UWB antenna for X-band applications.” Int. Symp. Adv. Electr. Commun. Technol. (ISAECT) 2019, 4, 78–82.

[79] Sanmugasundaram, R. Dileepan, D. Natarajan, S. “Design of CPW antenna for network applications.” Int. J. Eng. Technol, pp.2525–2527,2018.

[80] Sharma, A. Khanna, P. Shinghal, K. Kumar, “A Design of CPW-Fed Antenna with Defected Substrate for Wideband Applications.” J. Electr. Comput. Eng. 2016.

[81] Khanna, P. Sharma, A. Singh, A.K. Kumar, A. “A CPW—Fed octagonal ring-shaped wideband antenna for wireless applications. “Adv. Electromagnet. 2018.

[82] Quddious, A. Abbasi, M.A.B. Antoniades, M.A. ryonides, P. Fusco, V.; Nikolaou, S. “Dynamically Reconfigurable UWB Antenna Using an FET Switch Powered by Wireless RF Harvested Energy.” IEEE Trans. Antennas Protag. 2020.

[83] Jansari, D.V. Amineh, R.K. “A two-element antenna array for compact portable MIMO-UWB communication systems.” AIMS Electron. Electr. Eng. 2019.

[84] Simorangkir, R.B. Kiourti, A. Esselle, K.P. “UWB Wearable Antenna with a Full Ground Plane Based on PDMS-Embedded Conductive Fabric.” IEEE Antennas Wire. Protag. Lett. 2018.

[85] Negi, D. Khanna, R. Kaur, J. “Design and performance analysis of a conformal CPW fed wideband antenna with Mu-Negative metamaterial for wearable applications.” Int. J. Micro. Wire. Technol. 2019.

[86] Rusdiyanto, D. Apriono, C. Astuti, D.W.; Muslim, M. Bandwidth and Gain “Enhancement of Microstrip Antenna Using Defected Ground Structure and Horizontal Patch Gap”. Sinergi 2021.

[87] Lu, P. Song, C. Huang, K.M. “Ultra-Wideband Rectenna Using Complementary Resonant Structure for Microwave Power Transmission and Energy Harvesting.” IEEE Trans. Micro. Theory Tech. 2021.

[88] Kumar, T.R. Madhavan, M. “Design and Optimization of Wearable Microstrip Patch Antenna using Hybrid Fuzzy Flamingo Swarm Optimization Algorithm for RF Energy Harvesting.” Iran. J. Sci. Technol. Trans. Electr. Eng. 2022.

[89] Imran, A.I. Elwi, T.A.; Salim, A.J. “On the Distortion less of Uwb Wearable Hilbert-Shaped Metamaterial Antenna for Low Energy Applications.” Prog. Electromagnet. Res,2021.

[90] Kumar, M. Kumar, S. Jain, S. Sharma, A. “A Plug-in Type Integrated Rectenna Cell for Scalable RF Battery Using Wireless Energy Harvesting System.” IEEE Microw. Wire. Compony. Lett. 2022.

[91] Shi, Y. Jing, J. Fan, Y. Yang, L. Wang, M. “Design of a Novel Compact and Efficient Rectenna for WIFI Energy Harvesting.” Prog. Electromagnet. Res,2018.

[92] Mathur, M. Agrawal, A. Singh, G. Bhatnagar, S.K. “A compact coplanar waveguide fed wideband monopole antenna for RF energy harvesting applications.” Prog. Electromagnet. Res,2018.

[93] Ismail, N. Kadir, E.” A. Reversed L-type Matching Impedance of RF-to-DC Rectifier for Energy Harvesting System.” J. Electr. Electron. Syst. Res,2021.

[94] Valenta, C.R. Durgin, G.D. “Harvesting Wireless Power.” IEEE Microw. Mag. 2014.

[95] Q. M. Hamza, S. M. Nabil, M. Hassan, “International Symposium on Advanced Electrical and Communication Technologies,”2019.

[96] R. Hussain, M. S. Sharawi, A. “Shamim,” IEEE Transactions on Antennas and Propagation ,2018.

[97] K. A. Fante, M. T. Gemeda, Int. J. Electr. Comput. Eng. 2021.

[98] Y. M. Mohamed, H. Abdallah, E. EI-Hennawy, IEEE Access 7, 2019.

[99] R. Sanmugasundaram, D. Dileepan, S. Natarajan, International Journal of Engineering and Technology ,2018.

[100] D. Rusdiyanto, C. Apriono, D. W. Astuti, M. Muslim, 2021.

[101] A. Mithari, U. Patil, Int. Res. J. Eng. Technol,2016.

[102] M. K. Abdulhameed, M. S. M. Isa, I. M. Ibrahim, M. K. Mohsen, S. R. Hashim, M. L. Attiah, J. Adv. Res. Dyn. Control Syst,2018.

[103] D. Negi, R. Khanna, J. Kaur, International Journal of Microwave and Wireless Technologies 11(8), 806 (2019). [22] A. H. A. Al-Shaheen, ARPN J. Eng. Appl. Sci,2019.

[104] Nesasudha, M. "Microstrip antenna for early stage breast cancer detection—A survey." *Health and Technology* vol.11 , PP.1191-1204,2021.